NTNU – Trondheim
Norwegian University of
Science and Technology

Equipment and Production of Columnar Sea Ice Replica in NTNU Cold Lab

Thor Olav Myklebust

Master of Science in Physics and Mathematics
Submission date: July 2014
Supervisor: Arne Mikkelsen, IFY
Co-supervisor: Knut V. Høyland, BAT

Norwegian University of Science and Technology
Department of Physics

Sammendrag

Denne masteroppgaven omhandler en forbedring av en istank som blir brukt til produksjon av is på en kuldelab ved NTNU. Målet var å forbedre kontrollen av vanntemperautren i tanken. De gamle sensorene ble byttet ut med syv nye sensorer med en måleoppløsning på 0.1 °C. Det ble utviklet et dataprogram i LabVIEW som overvåket og kontrollerte temperaturen i tankens. For å kontrollere og stabilisere vanntemperaturen ble det brukt en P-regulator.

For å teste det nye varmesystemet ble tre isforsøk gjennomført. Et med ferskvannsis og to med havis. I disse testene ble temperaturutvikling og istykkelse studert.

Temperaturmålingene viste stabilitet, men det ble målt små lokale variasjoner på 0.1 °C i hver seksjon av tanken. Årsaken til dette var enten konveksjon i vannet, eller for dårlig kalibrering av sensorene. Den ene sensoren ble plasert så høyt på veggen at den ble dekt av is og målte derfor istemperatur.

Isen viste seg å være tykkere langs veggene, sammenlignet med midten av isflaket. Tykkelsen langs veggen viste seg å være mye mindre sammenlignet med observert isvekst fra forsøk som ble gjort før forbedringene av tanken. Det ble observert en forskjell i tykkelse fra vegg til vegg i tanken. Dette skyldtes muligens av tankens posisjon i kuldelaben.

Oppgaven har også sett nærmere på hvor mye sprayetid har å si for hvor store iskrystallene blir når man lager havis. Spraying blir gjort for å igangsette vekst av iskrystaller. Det ble gjennomført to tester, en med lang sprayetid og en med kort. Det viste seg at sprayetiden har mye å si for hvor store iskrystallene i isen blir. Størrelsen på krystallene fra testen med kort sprayetid viste seg å være ca. 1/3 av størrelsen til krystallene i isen med lang sprayetid.

Abstract

This Master's thesis considers an ice tank used for production of ice in a cold lab at NTNU. The goal was to improve the temperature control of the water in the tank. Original sensors were replaced with seven new sensors with a resolution of 0.1 °C. The temperature was controlled by a computer program made in LabVIEW. A P-controller was used to control and stabilize water temperature.

The system was modified and tested with three different experiments. One with production of freshwater ice and two with sea ice. The tests examined the temperature development in the tank and resulting ice sheet thickness.

The temperature measurements showed stability, but with small local variations of 0.1 °C which were consistent throughout every test. This was either caused by convective mixing or an insufficient calibration of sensors. Ice temperatures could also be measured after the modifications were done.

The ice was found to be thicker along the tank wall as expected, but less severely compared to observations made before the modifications. A comparison between the walls found a difference in thickness, and was probably caused by the location of the tank relative to the lab room's cooling system.

This Master's thesis also investigates how the time spent on spraying, for initiation of crystal growth, affects the crystal size when producing sea ice. Two tests were conducted; short and long spraying time. The results showed that the spraying time had a significant impact on the resulting ice structure. The grain size of the crystals from the short spraying test was $\approx 1/3$ of the grain size from the long spraying test.

Acknowledgement

This Master's thesis was written at NTNU Gløshaugen during the spring semester 2014. All experimental work was performed in the cold lab at the Faculty of Engineering, Science and Technology. The thesis is a result of 6 months of hard work, problem solving and freezing my butt off in the cold lab. Most of the literature was found by using the university's library system BIBSYS while some was provided by Knut V. Høyland.

I would like to express my gratitude to my supervisors Knut V. Høyland at the Department of Civil and Transport Engineering and Arne Mikkelsen at the physics department. Special thanks to Mr. Høyland who has guided me through the whole semester and has shown huge enthusiasm which has given me motivation to produce this paper you are reading now.

This master thesis would also not been possible without the great help and knowledge from Per A. Østensen. Thanks for the help of designing circuit boards, ordering components and most of all; lending me your workshop and equipment. I hope I didn't make too much of a mess in there.

I would also like to say thank you to Frank Stæhli and the carpenters at NTNU for helping me with mechanical work on the tank. Thank you to Nicolai Greaker for cooperating in the lab and pictures of experiment results. I have needed a lot of assistance in the cold lab due to a lot of heavy lifting and NTNU's HSE rules. For this Erik Lydersen, Anna Pustogvar, Morten Hatlen and Bjørn Johan Endresen has my gratitude for helping me. I could not have done this without your help.

Thanks to Lise Kalvø for giving me access to the instrumentation lab at department of physics. And finally my appreciation and thanks go to Bjørn Johan Endresen for proof-reading my report and helping me to finalize my Master's thesis.

Contents

Sammendrag i

Abstract iii

Acknowledgement v

Introduction 1

1 Background and motivation 3
1.1 The ice tank . . . 3
1.2 Motivation for modifying the tank . . . 4

2 Planning and development process 7
2.1 Discussion of solution . . . 7
2.1.1 Locally controlled . . . 7
2.1.2 Computer controlled . . . 8
2.1.3 Chosen system set-up . . . 8
2.2 Heating system and insulation . . . 10
2.2.1 Heating cables . . . 10
2.2.2 Insulation . . . 11
2.2.3 Relays . . . 12
2.3 Temperature sensor . . . 14
2.3.1 Platinum resistance thermometer . . . 14
2.3.2 Callendar-Van Dusen equation . . . 15
2.3.3 The selected sensor . . . 17
2.3.4 Wheatstone Bridge . . . 20
2.3.5 Designing and building amplifier circuit board . . . 22
2.3.6 Building sensors . . . 25
2.3.7 Creating Wheatstone bridges . . . 26
2.3.8 Mounting on tank . . . 27

2.3.9 Installing terminal box . . . 30
2.3.10 Errors and deviation . . . 30
2.4 Computer system . . . 32
2.4.1 Control engineering, P-I-D . . . 32
2.4.2 NI USB-6009 DAQ device . . . 33
2.4.3 LabVIEW . . . 34
2.4.4 LabVIEW program . . . 35
2.5 Calibration . . . 38
2.5.1 Calibration methods . . . 38
2.5.2 Calibration of sensors . . . 38
2.5.3 Calibration and testing of computer program . . . 39

3 Testing and Validation **45**
3.1 Sea ice structure . . . 45
3.2 Experiment procedure . . . 48
3.2.1 Preparations . . . 48
3.2.2 Thin sections . . . 48
3.3 Fresh water ice experiment . . . 52
3.3.1 Method . . . 52
3.3.2 Results . . . 52
3.4 Motivation to look at the spraying technique . . . 56
3.5 Sea ice experiment 1: Long spraying time . . . 57
3.5.1 Method . . . 57
3.5.2 Results . . . 57
3.6 Sea ice experiment 2: Short spraying time . . . 65
3.6.1 Method and data . . . 65
3.6.2 Results . . . 65

4 Discussion **73**
4.1 Measured temperatures and sensor readings . . . 73
4.2 Insulation . . . 75
4.3 Computer program . . . 75
4.4 Ice thickness . . . 76
4.5 Thin sections . . . 78

5 Conclusion **81**

6 Further work **85**

Bibliography **87**

A Appendix **89**
A.1 List of components and equipment used to modify tank 89
A.2 List of equipment 90
A.3 Pictures and data from Salt ice experiment 1 91
A.4 Pictures and data from sea ice experiment 2 101
A.5 Tank set up. Sensor position and wiring diagram 111

Introduction

The interest in the Arctic area is increasing, especially for its large hydrocarbon energy sources, its effective shipping routes and an increasing study of the global climate changes. The Arctic area is a rough environment with rapidly changing weather and presence of sea ice and icebergs is a continuous risk. Knowledge about these things and their effects is crucial to operate in these environments. Studies are being done in the Arctic area, but also at geographical locations where sea ice is not possible to come by. This makes it necessary to develop a method to replicate sea ice in cold labs.

This master's thesis is a continuation of the project assignment from fall semester 2013, *Properties and growth of laboratory made columnar saline ice*. The thesis will take a closer look on the equipment used in the production process of making sea ice replicas in the cold lab at NTNU.

The main focus will be the ice tank. There were discovered significant deviations in the temperature regulation in the tank during ice production last semester. The main goal is to improve the control system and quantify its effect on the ice production. The type of control solution and method will be discussed in this report as well as the work process.

When creating sea ice, spraying needs to be done to initiate columnar crystal growth. The project assignment *Properties and growth of laboratory made columnar saline ice* mentions how the speed of spraying might affect the ice crystal sizes. This hypothesis will also be examined as a production method of creating columnar sea ice in this thesis.

Due to a fire incidence in the neighbouring lab, the cold labs were closed from 24.5.2014 to 12.06.2014 and no testing could be performed during this time. The last results were made close up to the end of the master thesis, and the author hopes that the report does not bear affects of this.

1 Background and motivation

1.1 The ice tank

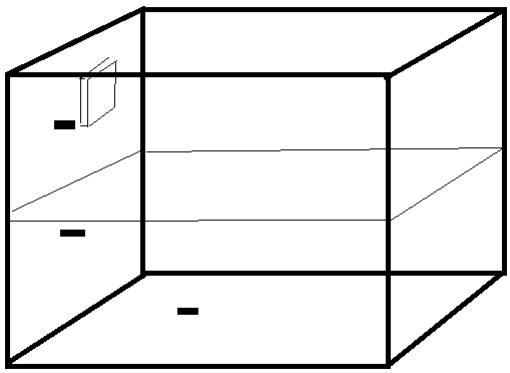

Figure 1.1: The previous ice tank set-up. Black rectangles indicate the position of the sensors.

Sea ice is used in a range of different studies; e.g. structure analysis, strength testing and model testing of structures planned to be build in ice affected areas. When replicating sea ice, the goal is to do the process as closely resemble as in nature. In nature sea ice is made due to cold air at the water surface, and the result is ice growing from above and downwards.

The tank is an open water tank. The inside walls made of stainless steel, re-

inforced by a thick metal rod surrounding the walls preventing the tank from exploding when full. The tank walls and bottom are installed with heating cables and isolated with Styrofoam. This to prevent ice from growing from the sides and the bottom. The heating cables are also meant to keep the water at or above freezing point so the tank doesn't deep freeze. The outside of the tank is covered with wood panels and the heating control system is located on the left wall (see fig. 1.1). This system makes the tank work well as an instrument to replicate sea ice in a cold lab.

The project assignment "*Properties and growth of laboratory made columnar saline ice*" looked at different techniques for growing sea ice in the ice tank. The results showed that the initial process was as much important as the equipment (the ice tank).

The tank is placed in a cold room where the room temperature can be controlled. The growth process is a slow process that takes several days depending on water salinity and temperature together with the air temperature in the lab.

1.2 Motivation for modifying the tank

The heating system in the ice tank is made out of 3 standard house floor heating systems which comes as an installation package with sensors and control system. They are separated into 3 sections; upper part of tank walls (top), lower part of tank walls (middle) and bottom part of tank (bottom). The control panel where the user sets the temperature was not sufficiently accurate. The temperature selector was a small wheel knob with a poor small-scale resolution. Also there was nothing to display the current temperature in the tank. All this made the current system inadequate to control the water temperature with a accuracy of 0.1 °C.

During experiments performed in the project assignment "*Properties and growth of laboratory made columnar saline ice*" several malfunctions were discovered. There was observed ice growth on the submerged parts of the tank walls during ice production. Also ice growth on the bottom of the tank was observed. This is an unwanted effect, which might affect the resulting structure of the ice at the surface.

Another anomaly observed was a faster ice growth at the surface along the tank walls compared with the middle of the surface [1].

The ice tank needs to be modified with better isolation and sensors with higher

accuracy as well as a control system where the user can monitor and control the water temperature in a resolution of 0.1 °C.

2 Planning and development process

2.1 Discussion of solution

The tank's water temperature is adjusted by the heat produced by the integrated heating cables in the walls and bottom, and by the cold air surrounding the tank. The water temperature is measured by sensors located inside the tank walls together with, but thermally separated from, the heating cables. The tank and the water it contains is defined as the *system* where the surrounding air is the environment affecting the system. The system needs to be controlled to regulate the temperature automatically by using control engineering. The system can be controlled by many different methods; two potential methods are locally controlled or computer controlled, from outside the cold lab.

2.1.1 Locally controlled

The old solution is a locally controlled solution. The control panel is mounted inside a small box on the outer tank wall. The control panel is three separate hardware units with an integrated control engineering system. This unit's only user input is temperature set point and it measures the temperature and controls the heating cables automatically. A potential improvement of this solution would be to replace the sensors with more accurate sensors, replace the control panel to also display the current temperature and the set point temperature as digital digits with a precision of 0.1 °C.

Few parts are needed due to the tank being locally controlled are and is therefore not a very expensive solution. It is also a simple solution which do not demand too much space. There are some disadvantages inherent to this solution. It will be hard or impossible to monitor the temperature development, which also makes

it hard to perform any logging of temperature. Performing any changes, if the system should act strange, is more difficult to execute on a programmed micro controller than in a computer software. There is also a lot of physical work done inside the cold lab, and a lot of tools are used, which may cause larger impacts on the control box that may lead to damaging the regulating system.

2.1.2 Computer controlled

This solution uses a computer to do the control engineering between the sensors and heating cables instead of a control panel at the tank wall. This solutions makes it possible to monitor and log the temperature development in the tank, which might be handy in post experimental work. The control engineering would be easier to calibrate due to it being performed in the computer software. This solution also presents the possibility to easily add new programs or applications to work with the tank, even adding instruments to the system.

The computer controlled solution is a more expensive solution since it demands a computer and a data acquisition device (analogue-digital/digital-analogue) so that the computer may communicate with the tank. It also depends on the reliability of the computer; If it shuts down, the heating system stops working. Other disadvantages with this solution is the requirement of more space than the local solution due to the computer's need to be located outside the cold lab.

2.1.3 Chosen system set-up

After evaluating both solutions its clear that the biggest potential is in the computer controlled solution. The possibility to log temperature information is useful when it comes to scientific research and documenting experiments. Also being able to combine these data with other data e.g. temperature measurements in the middle of the tank, is an interesting option. Figure 2.1 shows how the temperature control system works. A set temperature is given as user input to the computer program, whilst the computer reads the temperature measured by the sensors. The computer takes care of the control engineering and applies possible changes by sending information to the heating system in the tank, which executes the changes. This will again be measured by the temperature sensors and the information is then returned to the computer again. The surrounding cold air is characterized as a disturbance affecting the water in the tank.

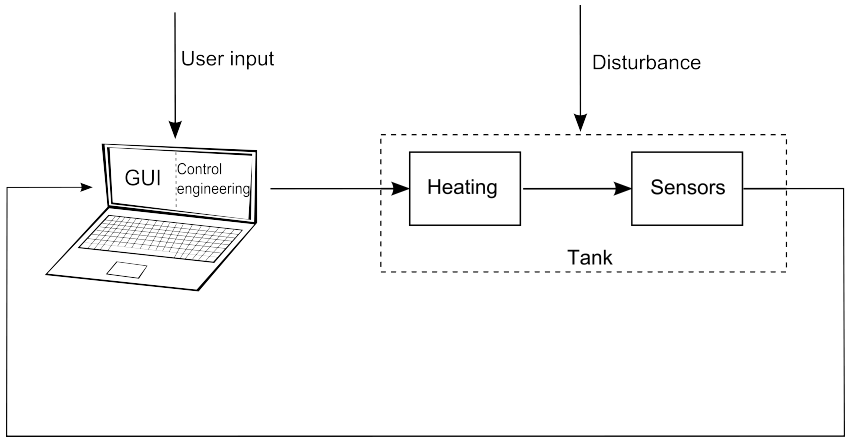

Figure 2.1: Temperature control system flow chart.

The computer controlled solution can be separated into 4 different parts (fig. 2.2), the computer system, temperature sensors, control engineering and heating system and insulation. These four parts will be addressed separately through this thesis, from theory to finished prototype.

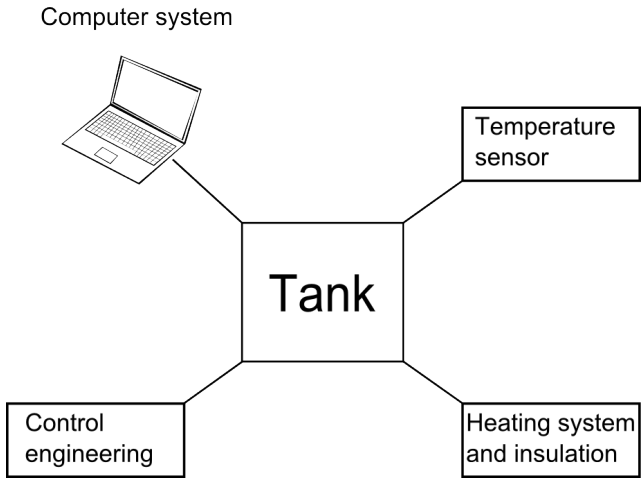

Figure 2.2: All parts representing the system.

2.2 Heating system and insulation

The submerged ice growth that was observed during ice production needed to be investigated. Some thoughts on the reason for this growth was that the heating cables was not distributed over the walls well enough. The tank walls needed to be opened for further investigation. After dismounting the outer panels, the problem was soon discovered. A thick steel rod was mounted on the middle all around the tank to prevent the tank from expanding when filled with water. This metal rod was not isolated from the outside and therefore worked as a heat conductor from the tank out to the surroundings. An old draining pipe was installed in the bottom of the tank, which caused good conditions for submerged ice growth due to the metal's high heat conductivity.

2.2.1 Heating cables

Figure 2.3: Heating cables on tank walls covered with aluminium tape, upper and lower seciton separated by the metal rod.

The heating cables are designed to be used as house floor heating and are driven by a regular 220 V power outlet. They are made out of a two-core cable with shielding and can be cut to desired length. The output effect from the cables are

approximately 6 W per meter cable. Since the task in hand was a modification of already installed heating cables, and the submerged ice growth was not caused by their position, was no repositioning of the cables needed.

The heating cables are divided into three parts, each heating their own area (upper walls, lower walls and bottom). The upper and lower sections are separated by a thick metal rod. The heating cables are wrapped around the tank and attached using metal tape. This is so the heat from the cables is distributed as well as possible over the wall. The cables at the wall are distributed in a distance from each other that the metal tape leaves no gap resulting in the metal tape covering all the wall surface, except the metal rod in the middle. The tank wall with the mounted heating cables is depicted in figure 2.3, where the metal rod can be clearly seen.

The bottom heating cable is located under the tank. It is not attached to the tank, but integrated in a wooden plate on which the tank stands. The cable is mounted in a zig zag pattern which has been milled out and then been covered with metal tape (see fig. 2.4). As seen in the figure, the gap between the heating cables in the bottom is much larger and therefore has ample space for placing new sensors.

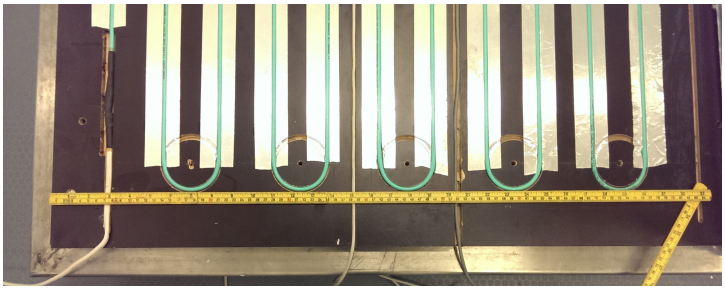

Figure 2.4: Bottom heating cable mounted in a zig-zag pattern.

2.2.2 Insulation

To avoid heat leakage and to minimize disturbance from the surroundings, the walls and the bottom plate are insulated with Styrofoam. This is shown in figure 2.17 where parts of the tank wall is covered with such. It also shows the metal rod not being covered by any insulation, which was the main reason for the submerged ice growth on the walls. The solution to this problem was adding more insulating material. Styrofoam is an ideal insulating material, due to its compact air-free structure and waterproofness which is convenient when work-

ing in a potentially wet environment. But Styrofoam could only be obtained in thicknesses of 50 mm, and since the wanted thickness was 2 cm another type of polystyrene had to suffice. This polystyrene contained a higher amount of air and was not as waterproof as Styrofoam, but was still a good thermal insulator. The old wooden panels covering the tank did not fit after adding more insulating. Cutting and mounting of new panels were done by the help from NTNU's carpenters. These panels also worked as thermal insulation, but more as protection for the polystyrene inside the walls. The old drain pipe was removed, the hole was sealed and covered with insulation.

2.2.3 Relays

A relay is an electric switch controlled by an electric signal. Usually a smaller voltage signal is used to switch the on-off state of the relay. The control signal and operating signal is isolated from each other. Relays are used in many applications e.g. large lighting systems or electrical motors.

The most common relay is mechanically switched. The control signal induces a magnetic field which moves a pin that closes the switch for the operating signal. When the control signal is turned off a spring will remove the pin and the switch is open. A mechanical relay has an estimated life span of 10^5 operations, making it sufficient in many applications where the frequent switching is not necessary [2].

The solid state relay (SSR) is a more modern relay, using semiconductors. The relay is switched by the small electrical signal lighting an LED, which triggers a light sensor to close the switch. The control signal operates the LED and when it is turned off the switch will change state to open. SSRs has a much longer life expectancy than mechanical relays due to no moving parts. The time it takes to lit the LED determines the switching speed of a SSR. This makes it much faster than a mechanical relay. The controlling and operating signal in an SSR can be both a DC and AC signal, depending on model. SSRs may generate electrical noise due to sudden switching in the AC signal. Some SSRs compensates with this problem by only switching when the AC sine wave is at zero voltage. This method is called "zero-voltage switching"[2] and therefore limits the relay to only switch 100 times in one second, when operating with a 50 Hz AC signal(a signal passes zero twice during one period).

Solid state relays was used to operate the new heating system. This due to their fast switching speed and long reliability. Instead of operating the heating cables with voltage regulation, the cables are operated by a rapid on-off function. This means that instead of letting the cables give e.g. 50% all the time, they

give 100% for half a second and zero for the rest. This solution is dependent on a relay that is stable and switches fast. Also to avoid generating electrical noise is "zero-voltage switching" used. For this application is a Crydom ED24D3 [3] used. With its DC control voltage range of 3-15 V and operating AC signal range of 24-280 V, the Crydom relay is ideal for this application. The relay is operated by a boolean signal sent from the computer program.

2.3 Temperature sensor

Temperature sensors can be divided into two groups; types that measures temperature and types that give a binary output when a given threshold is passed (e.g. thermostat) [2]. There are several different types of temperature sensors, using different measurement technology. All these methods have some strengths and weaknesses, some have high shock resistivity, some have higher measurement accuracy than others and some perform slow readings. This makes it dependent on the task in hand when it comes to determining type of sensor to use.

2.3.1 Platinum resistance thermometer

The electrical resistance in all conducting material changes with temperature. This variation is approximately linear for metals, which makes them convenient for temperature measurements. The temperature is calculated by measuring the resistance in the metal and comparing it with known values of resistance at a given temperature. A much used metal for this application is platinum, known as platinum resistance thermometers, PRT, (see fig. 2.5). They perform rapid readings, fast change of resistance, and have a good measurement accuracy. PRTs are able to measure in the range from approximately -150 ° to 1000 °C, depending on coating. But they also have poor sensitivity, which means that the change of resistance is very small over temperature and therefore high precision readings are needed. They are also shock sensitive due to the nanometre-thin platinum wires which changes resistance with temperature.

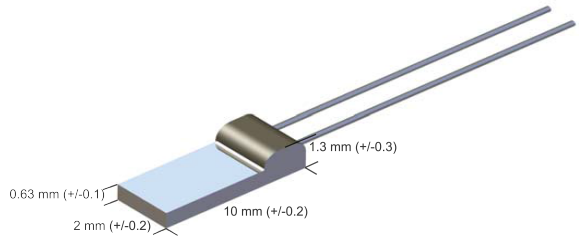

Figure 2.5: Platinum resistor thermometer.

Platinum sensors are most accurate at temperatures around their reference point, R_0, which is at 0 °C. At this point the resistance is typically 100 Ω or 1000Ω and are called PT100 or PT1000, respectively.

The PRT sensors are bound to follow the international standard called IEC751(DIN/IEC-60751). This standard separates the sensors in two classes; Class A and Class B,

though the industry uses two more classes; 1/3DIN and 1/10DIN. These industry classes have 1/3 and 1/10 the accuracy of class B, meaning that they are three and ten times more accurate then class B sensors. The accuracy tolerance for each class allowed by the standard is

$$\begin{aligned} \text{Class A} &= \pm(0.15 + 0.002 \cdot T)\ ^\circ\text{C} \\ \text{Class B} &= \pm(0.30 + 0.005 \cdot T)\ ^\circ\text{C}. \end{aligned} \tag{2.1}$$

The expressions in equation 2.1 states how much the temperature measurements may deviate from the actual temperature. And by studying these expressions it is clear that the sensors have the highest requirements to deviation at 0 °C (±0.15 °C Class A and ±0.3 °C Class B) supporting that the sensors are most accurate at their reference point.

Same applies to the industrial classes 1/3DIN and 1/10DIN, but with higher requirements to temperature accuracy. ±0.1 °C for 1/3DIN and ±0.03 °C for 1/10DIN at 0 °C (from eq. 2.2).

$$\begin{aligned} 1/3\text{DIN} &= \pm\frac{1}{3}(0.3 + 0.005 \cdot T)\ ^\circ\text{C} \\ 1/10\text{DIN} &= \pm\frac{1}{10}(0.3 + 0.005 \cdot T)\ ^\circ\text{C} \end{aligned} \tag{2.2}$$

2.3.2 Callendar-Van Dusen equation

The British physicist Hugh Longbourne Callendar experimented on the relation between resistance and temperature in platinum resistance thermometers(PRT). By performing measurements in phase transitions of known substances the expression known as Callendar equation was derived

$$R(T) = R_0\left(1 + A \cdot T + B \cdot T^2\right), \tag{2.3}$$

where R_0 is the value of the reference resistance at ^{0} ∘C and T is the measured temperature given in °Celsius. The constants A and B were empirically found from measurements of the phase transitions.

The Callendar equation (eq. 2.3) was later found imprecise at temperatures below −40 °C. This proceeded to the equation being redefined by M.S. Van Dusen in 1925 [4] to apply at temperatures below zero degree Celsius. The new expression was called the Callendar-Van Dusen equation.

$$R(T) = R_0\left[1 + A \cdot T + B \cdot T^2 + C(T - 100)T^3\right] \tag{2.4}$$

where R_0 is the value of the reference resistance at 0°C, T is the measured temperature given in °Celsius and A, B and C are the Callendar-Van Dusen constants calculated from

$$\begin{aligned} A &= \alpha + \frac{\alpha\delta}{100} \\ B &= \frac{-\alpha\delta}{100^2} \\ C &= \frac{-\alpha\beta}{100^4}. \end{aligned} \tag{2.5}$$

The constants α, δ and β are empirically found, some from predefined temperature points.

$$\alpha = \frac{R_{100} - R_0}{100 + R_0} \tag{2.6}$$

where R_{100} is the resistance measured at the boiling point of water and R_0 is the resistance measured at 0 °C. Further are δ and β defined as

$$\delta = \frac{R_0[1 + \alpha(260)] - R_{200}}{4.16 R_0 \alpha} \tag{2.7}$$

$$\beta = \begin{cases} const. & , T < 0\ ^\circ\mathrm{C} \\ 0 & , \text{else.} \end{cases} \tag{2.8}$$

δ is determined by another fixed point at high temperatures, *"When δ is determined from observations at the boiling point of sulfur, the temperature scale defined by the Calendar equation is indistinguishable from the thermodynamic scale in the range -40 ° to 600 °"* [4]. The last constant β is determined by a fixed point near the boiling point of oxygen (-182.96 °C).

The Callendar-Van Dusen constants for the chosen sensor for the tank are found to be $A = 3.9083 \cdot 10^{-3}\mathrm{C}^{-1}$, $B = -5.775 \cdot 10^{-7}\mathrm{C}^{-2}$ and $C = -4.183 \cdot 10^{-12}\mathrm{C}^{-4}$.

Equation 2.4 must be solved by respect to temperature, T, when calculating temperature from the measured resistance. This is a challenging task due to the equation being a fourth order equation. The original Callendar equation (eq. 2.3) is a second order equation and is much easier to solve with respect to temperature. The difference between these two equations is the term including the constant C. The contribution from this term is insignificant when looking at temperatures near zero degrees Celsius. This makes it preferable to use Callendar equation (eq. 2.3) instead of Callendar-Van Dusen (eq. 2.4) since the sensors application area is going to be close to this range. These two equations are plotted together in figure 2.6 in the temperature range of -200 ° to 200 °Celsius to investigate the

difference between them. By looking at the graph it is clear that the difference between the two equations are insignificant right below zero degrees Celsius.

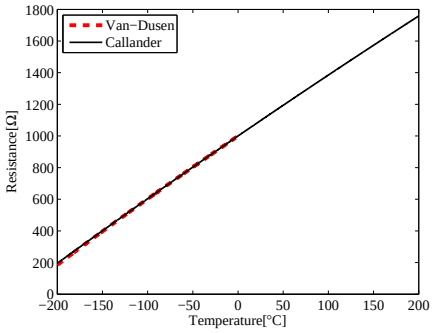

Figure 2.6: Callendar VS Callendar-Van Dusen.

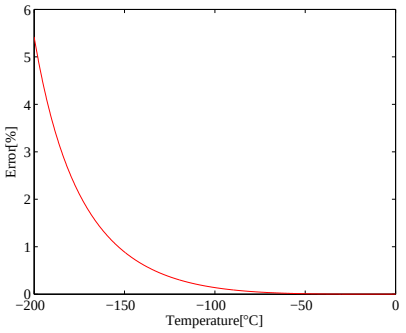

Figure 2.7: Error in Callendar equation.

Figure 2.7 shows the error development in the Callendar equation at lower temperatures, compared with Callendar-Van Dusen equation. The error reaches 1% first at -150 °C which states that the C evolving term is insignificant at temperatures around zero degrees Celsius.

This results in solving the Callendar equation (eq.2.3) with respect to temperature, which gives

$$T = -\frac{A}{2B} \pm \frac{\sqrt{A^2 - 4B(1 - \frac{R_x}{R_0})}}{2B} \tag{2.9}$$

where constant A and B are the Callendar-Van Dusen constants, R_0 is the reference resistance at 0 °C and R_x is the measured resistance over the sensor at temperature T. And since the $T = 0$ °C when $R_x = R_0$ is the final term of the relation between temperature and resistance in a PRT sensor

$$T = -\frac{A}{2B} + \frac{\sqrt{A^2 - 4B(1 - \frac{R_x}{R_0})}}{2B}. \tag{2.10}$$

2.3.3 The selected sensor

The wanted resolution of the temperature measurements in the tank is set to be of 0.1 °C. This makes the platinum resistance thermometers ideal. Though they are sensitive to shock, is this not a problem since they are being mounted inside the tank walls and are therefore well protected. Hence, direct impact on

the sensors' location on the inside walls may cause damage, but the probability of this event is insignificant.

The chosen sensor for the tank is a platinum sensor with a reference resistance, $R_0 = 1000\ \Omega$, named PT1000. The sensor with the biggest measurement surface was chosen and is shown in figure 2.5. Some other specifications are listed in table 2.1.

Table 2.1: Specification PT1000 [5]

Name	Value
Temperature coefficient (TCR)	3850 ppm/K
Temperature range	-200 °C to $+600$ °C
R_0	1000 ohm
Length	10.0 ± 0.2 mm
Width	2.0 ± 0.2 mm
Height	1.2 ± 0.3 mm
Response time(water)	$t_{0.5} = 0.33$ sec
Class	1/3 DIN

The PT1000 sensor has a temperature dependence of resistance according to IEC 60751 standard, which uses the Callendar Van-Dusen equation (eq. 2.4) to explain the relation between the resistance in the sensor and temperature (see sec. 2.3.2). The Callendar Van-Dusen equation is dependent on three empirical constants, which are found by solving the equation at three different known temperatures. For the chosen sensor are these constants found to be

$$\begin{aligned} \mathrm{A} &= 3.9083 \cdot 10^{-3}\ \mathrm{C}^{-1} \\ \mathrm{B} &= -5.775 \cdot 10^{-7}\ \mathrm{C}^{-2} \\ \mathrm{C} &= -4.183 \cdot 10^{-12}\ \mathrm{C}^{-4}. \end{aligned} \tag{2.11}$$

Due to the temperature range of this application, the Callendar Van-Dusen equation is replaced with the Callendar equation (see sec. 2.3.2).

In the original version of the tank system were there sensors used. One for each heating cable (see fig. 1.1). This configuration of sensors is sufficient enough for controlling the water temperature, but adding more sensors gives a opportunity to investigate the conditions in the tank more closely during ice production.

The new set-up is with seven sensors, five placed on a vertical line on the wall

and two on the bottom, as shown in figure 2.8. This makes it possible to create a vertical temperature profile.

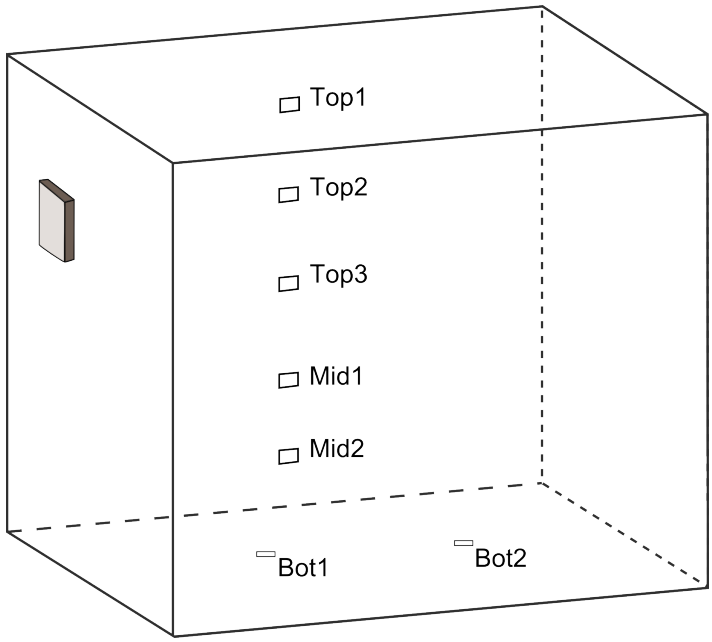

Figure 2.8: Location of new sensors.

2.3.4 Wheatstone Bridge

A Wheatstone bridge is an electrical circuit used to measure a unknown resistance of an electrical component [6]. It is made out of three high precision resistors (R_{1-3}) and a unknown resistor R_x, distributed in two parallel circuit branches (see fig. 2.9). A highly accurate voltage detector, V_{AB}, is placed between the junction points A and B, as a bridge, to measure any potential difference between these two points.

The originally way to use the Wheatstone bridge was to place the unknown resistor, R_x, in the circuit and adjust the value of R_2 and R_3 until no current went through the voltage detector (V_{AB}) [7]. Then the bridge would be "balanced" and the unknown value could be calculated by using Kirchhoff's laws and the values of R_1, R_2 and R_3.

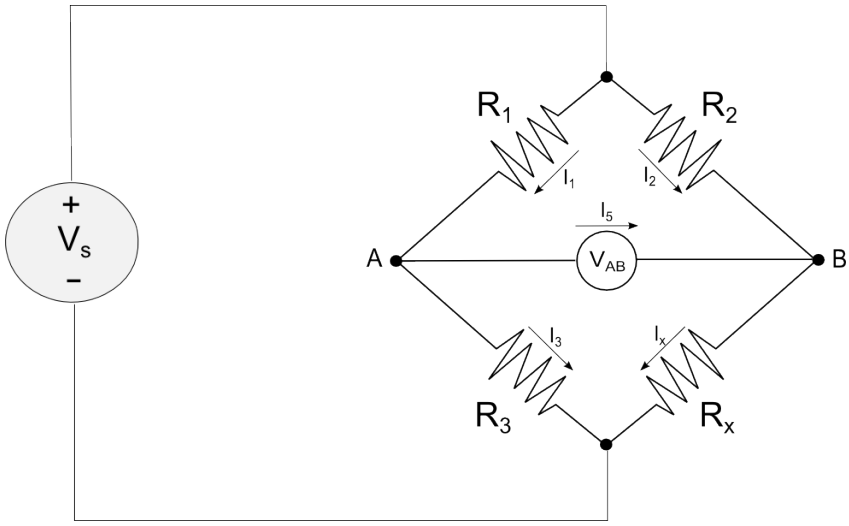

Figure 2.9: Wheatstone Bridge.

The value of resistor R_x may also be found without balancing the bridge. It can be calculated if the values of the resistors R_{1-3} and the potential difference between the junction points (A-B) are known. An expression to calculate the unknown resistance of R_x may be derived by using Ohm's law and by considering the junction points as potential dividers.

Starting with applying Ohm's law

$$V = R \cdot I \tag{2.12}$$

on the right branch in the circuit in figure 2.9.

$$V_s = I \cdot (R_2 + R_x). \tag{2.13}$$

The electrical potential in the junction point B is defined as

$$V_B = I \cdot R_x. \tag{2.14}$$

Inserting this in respect for I in equation 2.13 gives

$$V_B = \frac{V_s \cdot R_x}{(R_2 + R_x)}. \tag{2.15}$$

Applying the same on the left branch;

$$V_A = \frac{V_s \cdot R_3}{R_1 + R_3}. \tag{2.16}$$

The potential difference between the junction points A and B is expressed as

$$V_{AB} = V_A - V_B. \tag{2.17}$$

Inserting for the expressions above gives

$$V_{AB} = \frac{V_s \cdot R_3}{R_1 + R_3} - \frac{V_s \cdot R_x}{R_x + R_2} \tag{2.18}$$

and rearranging this expression with respect to R_x, gives

$$\begin{aligned} R_x &= \frac{R_2(\frac{R_3}{R_1+R_3} - \frac{V_{AB}}{V_s})}{1 - \frac{R_3}{R_1+R_3} + \frac{V_{AB}}{V_s}} \\ &= \frac{R_2}{\frac{(R_1+R_3)V_s}{R_3 \cdot V_s - V_{AB}(R_1+R_3)} - 1} \end{aligned} \tag{2.19}$$

So, by measuring the potential difference, V_{AB}, over the bridge, it is possible to calculate the values of the unknown resistance R_x of a PRT sensor by using equation 2.19.

2.3.5 Designing and building amplifier circuit board

The signals from the Wheatstone bridges are quite weak, and are not ideal to travel through a signal cable over long distances. This is because small voltage signals are easily affected by noise and interference from the surroundings. Countermeasures for these effects are isolating the signal cables and amplifying the signal. The signal is amplified by using an instrumentation amplifier, INA125 [8] and INA126 [9], produced by Burr Brown Corporation.

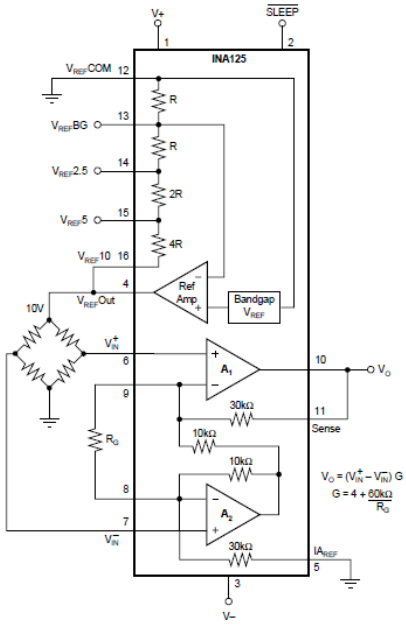

(a) INA125 [8].

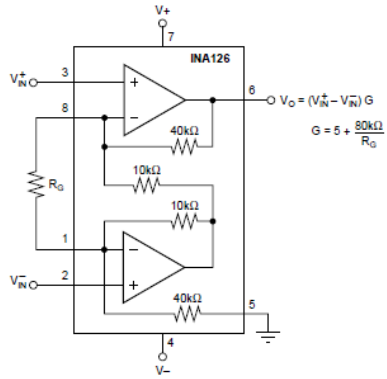

(b) INA126 [9].

Figure 2.10: Instrumentation amplifiers.

There are seven different sensor signals from seven Wheatstone bridges that needs to be amplified, which is done by using one of INA125 (fig. 2.10a) and six of INA126 (fig. 2.10b). These two components are almost identical, but together with the amplification circuit the INA125 also has a circuit creating a reference voltage signal. This voltage is a reference voltage to power every Wheatstone bridge. This reference voltage is the same as V_s in figure 2.9. The Wheatstone bridge is also visible in the left side of figure 2.10a. Since the INA125 powers the Wheatstone bridges does the INA126 only read two signals (V_{in}^+ and V_{in}^-). V_{in}^+ is

connected to the junction point A and V_{in}^- to junction point B in figure 2.9. The component amplifies the voltage difference between these two signals and returns it as one output, denoted as V_{AB} in figure 2.9 and V_o in figure 2.10b.

The two instrumentation amplifiers have different gain calculations, which are determined by the used gain resistance, R_G. The formulas are visible in both figures in figure 2.10, denoted as G. Due to the limits of the data acquisition device it is only capable of reading voltage signals in the range of -10 to +10 V. This results in the size of the gain determining the temperature range that can be measured. The resulting measurable temperature scale are listed in table 2.2.

Table 2.2: Results from amplified signal

Component	INA125	INA126
Resistance(R_G)	200 Ω	200 Ω
Gain	304	405
V_{Max} read from sensors	±0.0328 V	±0.02469 V
Temperature range	-25.69°/+28.88°C	-19.56°/+21.33°C

The measurable temperature range resulting from the amplified signal is in the range ≈ -20 ° to +20 °C, or larger, which is an appropriate measurable temperature range. Any larger range demands lower gain, which could result in noise disturbances in the signal.

All components had to be soldered on a strip board, but before doing this a sketch of the circuit board showing the position of all components relative to each other had to be made. The design of this sketch was done by Per A. Østensen, he also helped with the selection and ordering of components to be used in the circuit.

The design of the amplifier circuit is shown in figure 2.11. The circuit was powered by a 5 V source that was amplified to ±12 V, using a DC/DC converter from Traco Power which is located in the top of figure 2.11.

The seven output groups to the left in figure 2.11 are connection points for the sensors, and the amplified signal output to be sent to the computer is located on the right side, denoted "Out1-7". Other inputs are a +5 V signal and a ground signal, these are given from the computer's data acquisition device. The gain resistors was placed on the back side of the board, to save space, and is not located on the front as the sketch indicates. The finished signal amplifier circuit board is depicted in figure 2.12. In this picture the circuit sensor connections are seen

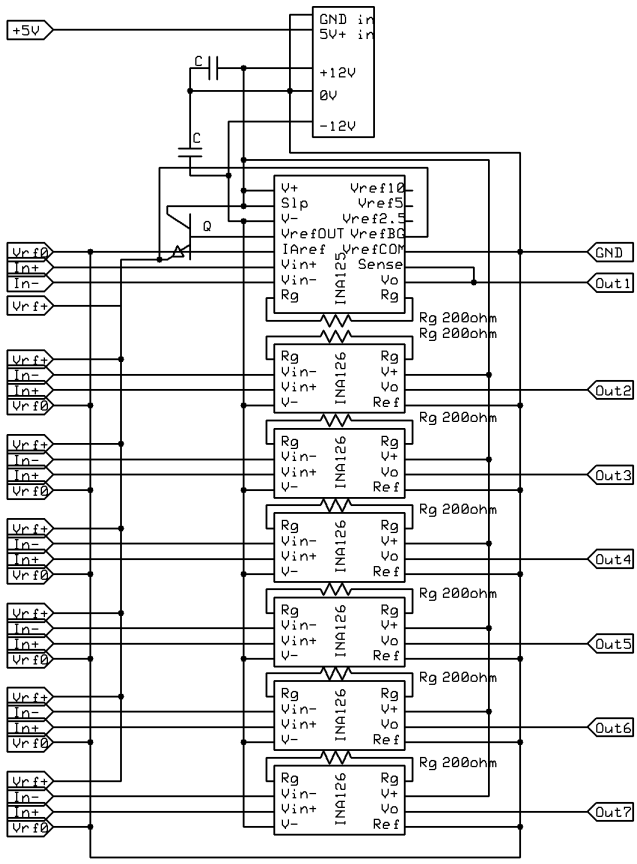

Figure 2.11: Sketch of amplifier circuit board, done in "ExpressSCH" [10].

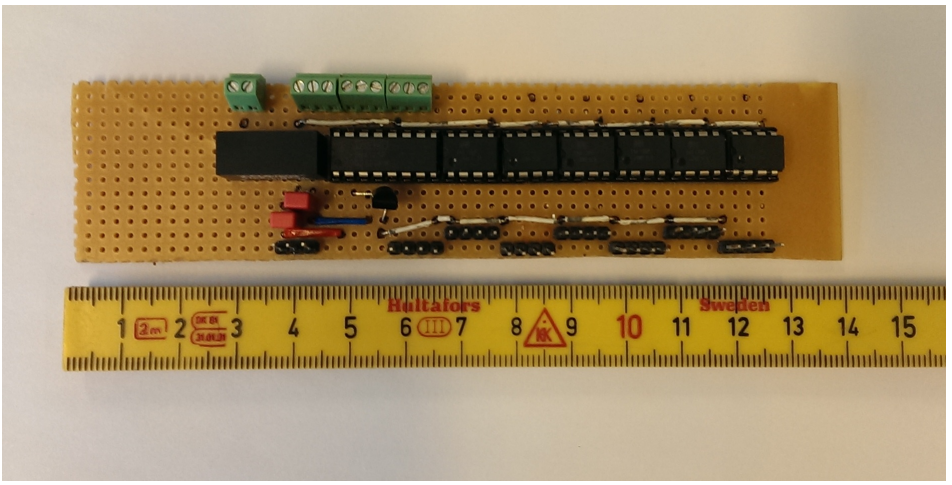

Figure 2.12: Finished amplifier circuit board.

at the bottom, and the amplified output signals at the top. They are grouped together by the green connection channels in the top left of the circuit board. These are mounted on to easily attach the signal cables by use of a screwdriver. The sensors are also easily connected by the use of molex plug connectors. The sensor signal cables are fixed with terminal pins which are then attached to a molex socket. This socket can easily be connected to the sensor pins located in the bottom of the picture in figure 2.12.

All soldering and wiring was done in the instrumentation lab at the department of physics and at Per Østensen's workshop. The reason for the board being longer than the circuit itself is that it can be easily installed in the terminal box.

2.3.6 Building sensors

The PT1000 sensors are small in size, and their connection wires are very fragile which results in the PT1000 sensors not being very suitable to be mounted directly on the tank wall. This was solved by attaching the sensor to a separate aluminium plate and encapsulating it inside a plastic cap for protection.

Aluminium was chosen due to its high thermal conductivity properties (see tab.2.3) so the rapid temperature changes between the tank and sensor were maintained. The sensor was glued to the aluminium plate with two-component glue. This glue was resistant to movement, due to being primarily made for straining gauges. The

surface dimensions of the aluminium plate was 35x35 mm and had a thickness of 1 mm. It is depicted in figure 2.13. It was important that the metal used for the sensor not affected the speed of the temperature change.

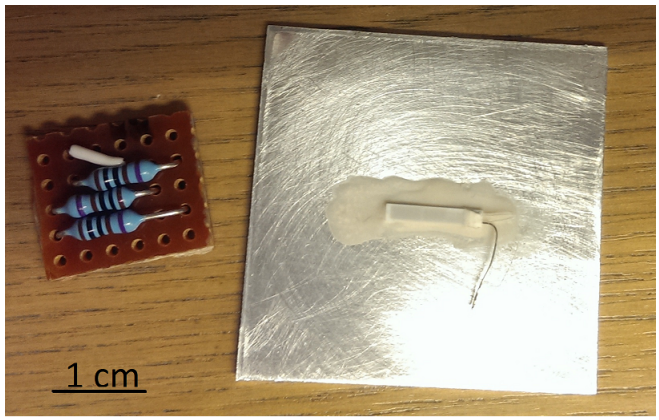

Figure 2.13: Wheatstone bridge together with the PT1000 glued to aluminium plate.

Due to the weak wires of the PT1000, small soldering stickers were also glued to the aluminium plate. These are flexible stickers with conducting metal on them, working as a connection pad for two wires. It was used to solder the PT1000 wires in one end and the connecting wires to the Wheatstone bridge in the other end. The wire distance between the sensor and the bridge was very short so they were both encapsulated together into a little black plastic cap, dimensions 25x25x15mm. The empty air in the cap was filled with *BT Multibond rapid* [11], which was electrically insulating paste chosen to prevent short-circuiting and to glue the cap to the aluminium plate. A small hole was drilled in the cap so that the signal cable connected from the Wheatstone bridge to the amplifier circuit could fit. The sensor unit now consists of; the Wheatstone bridge, PT1000, aluminium plate and a plastic cap and together are depicted in figure 2.15.

2.3.7 Creating Wheatstone bridges

The Wheatstone bridges was built according to the sketch shown in figure 2.14. The circuit has six connection points; Vrf+ is the reference voltage of 1.2 V, Vrf0 is ground, In+ is junction point A and In- is junction point B. The voltage difference between these to junction points, (In+ - In-) is the signal to be be amplified before being sent to the computer data acquisition device. The two last points is where the PT1000 sensor was connected since it could not be located on the

circuit board.

The bridge is built on a strip board and is made out of three precision resistors, all in the size of 1000Ω, which are attached by soldering. The PT1000 is attached to the circuit by soldering the wires that are connected to the aluminium plate, where the PT1000 is located. One of the resulting bridges can be seen in figure 2.13, before connection of cables and wires.

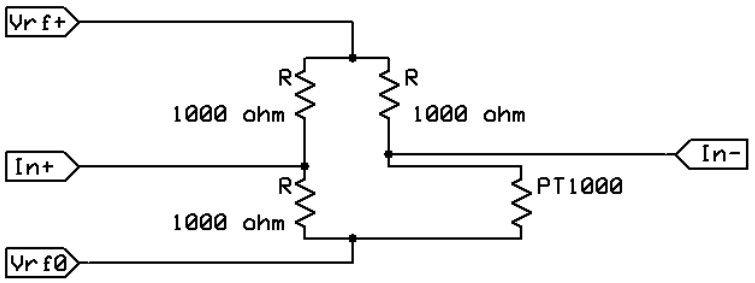

Figure 2.14: Schematic of Wheatstone bridge.

The signals Vrf+, Vrf0, In+ and In- are all sent trough a four-core cable with shielding to prevent noise and interference. All signal cables are connected to the amplification board, located in a terminal box on the outside of the tank wall. The cable is shown, connected to a sensor, in figure 2.15.

2.3.8 Mounting on tank

The sensor unit was glued on the tank wall, as depicted in figure 2.15. The glue had to be able to handle low temperatures and thermal expansion since the temperature change in the room could be up to 60 °C. Aluminium and steel have different thermal properties, which could create tension in the glue holding the sensor unit. Their respective expansion values are listed in table 2.3. The chosen glue for the task was an industrial type called Loctite 480 [19]. A low viscosity, one-component, glue that needed sparse application to attach the sensors to the tank wall. The thermal conductivity of this glue was not especially high, but due to the thin layer it constituted between the tank steel and the sensor's aluminium plate was its affects on the temperature readings considered negligible.

Figure 2.15: A finished sensor glued to the tank wall, located between aluminium tape covered heating cables.

The heating cables are mounted with aluminium tape, this had to be removed in the area where the sensor unit was mounted. Not doing this would affect the temperature readings due to heat from the cables.

Table 2.3: Material properties.

Material	Thermal conductivity $[\frac{W}{m \cdot K}]$	Thermal expansion Volume$[\frac{\mu m}{m \cdot K}]$, (20°C)	Thermal expansion linear $[\frac{\mu m}{m \cdot K}]$, (20°C)
Water	0.58	207	69
Stainless steel	13 - 16	51.9	17.3
Glue(Loctite)	0.1		80
Aluminium	205	23.1	69

The sensor placed under the bottom of the tank was not glued to the tank. Instead two holes were carved out in the bottom plate where the heating cables were integrated. The sensors were placed in these holes deep enough to just barely be above the surface of the bottom plate. The signal cables were placed in a milled track in the plate, so the weight of the tank wouldn't cause damage. One of the integrated sensors in the bottom plate is depicted in figure 2.16.

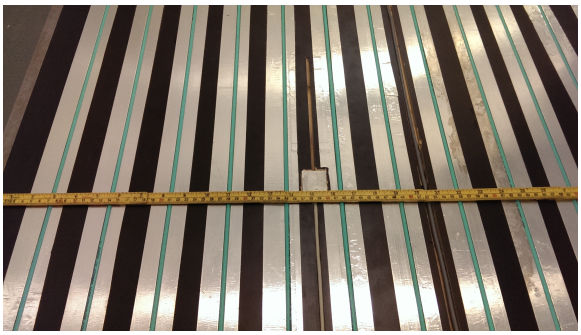

Figure 2.16: Sensor integrated into the bottom plate of the tank

The other five sensors were placed on a vertical line on one of the tank walls (fig. 2.17 and 2.8), so a temperature profile could be made. A consistent distance between the sensors could not be achieved due to the positioning of the heating cables. The sensors positions are listed in the appendix A.5.

Figure 2.17: Five sensors in vertical line measuring vertical temperature profile in the tank.

2.3.9 Installing terminal box

After mounting on all the sensors, they were then wired to the amplifier circuit board. The circuit board was placed inside a metal box that was mounted on the outside wall. Together in this terminal box were the relays to control the heating cables installed (see fig. 2.18). There are two cables attached from the outside to this terminal box; one signal cable connected to the computer data acqusition device and one 220 V electricity cable which was connected to the relays to power the heating cables. From the inside of the terminal box were the sensors and heating cables connected. Since the terminal box is not to be opened regularly was it sealed with a lid so non of the fragile components or cables are exposed to the surroundings.

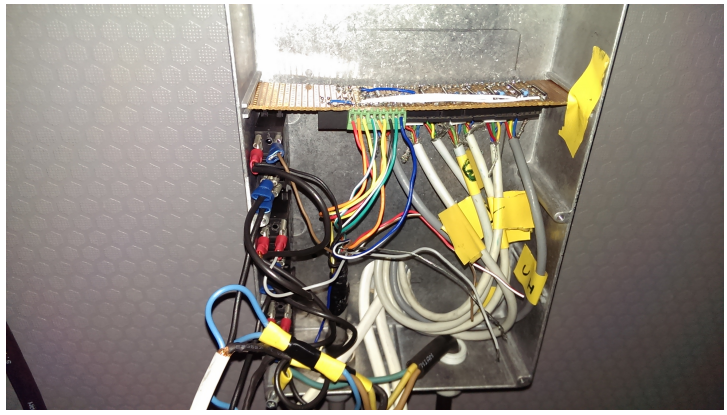

Figure 2.18: Terminal box with amplifier circuit and heating cable relays.

2.3.10 Errors and deviation

There are several things that can cause misreadings of the temperature from the point it is measured to the point where it is calculated. Most of these things are not a potential case in this thesis, but is worth mentioning.

A known effect causing misreadings in temperature measurements is hysteresis. This effect happens due to large rapid temperature changes. When a sensor measures a temperature and suddenly the temperature changes considerably it may measure a higher or lower temperature than actual, depending on the direction of the changing temperature. The possibility for hysteresis occurring in the tank is negligible, due to slow temperature variations and the small range of temperature.

The signal cables are located together with the heating cables, which are turned on and off frequently. This may generate noise, affecting the sensor signals travelling through the signal cables. This is prevented by using signal cables with shielding. Shielding is a metal wrapping inside the signal cable covering the actual cables located in the center. This causes any generation of noise to happen in the outer lying shielding instead of the cables carrying the signals. Though "zero-voltage switching" is applied when turning the heating cables on and off may this not be enough to completely remove all chances of noise occurring.

After installing the whole system and testing it with the computer program, a small deviation was discovered in the signal cable from the terminal box to the computer data acquisition device. A signal loss of 0.15 V was detected. This was not expected since approximately no current was going through the cable. After further examination it was determined that the ground cable was too small for the amplifier circuit board. By adding a second and separate ground cable to the DC/DC converter and a second and third cable for the +5 V signal the deviation was terminated. The result of these changes was a 0.4 °C higher temperature readings in the computer software. Due to this the previous sensor calibrations were no longer valid. This anomaly was discovered late in the process and there was no time to do a proper recalibration, so a second string was to perform a comparison calibration. This was done by stirring the water well and measuring the temperature with an external temperature gauge, and then calibrate the sensors according to its readings.

2.4 Computer system

2.4.1 Control engineering, P-I-D

A system that is affected by the surroundings (e.g. volume change, vibrations, pressure and temperature) needs to adjust its self according to these changes to remain stable. This is done with control engineering. Control engineering have been a key in modern society where machines and systems are more and more common.

The system to be controlled must be defined when using control engineering. The system is what needs to be controlled, while the surroundings are the disturbances affecting the system. Which causes the system's need to be controlled.

The water temperature in the tank needs to be kept at a predetermined temperature. Control engineering is used to achieve this. The water temperature is measured by placing temperature sensors on the outside of the tank walls. The walls are also covered with heating cables and insulating material, to prevent as little heat as possible to fluctuate from the cables to the surroundings. The insulation also prevent outside temperature disturbing the heating.

Feedback and feed-forward
There are two ways to perform control engineering; by feedback- or feed-forward coupling [12]. To use feed-forward the error affecting the system is measured and the control engineering compensates with this disturbance before it happens. Feedback measures the current situation and compares it with the wanted state. The difference between these states is used to affect the current state. This is the most used method and is the method of choice to control the water temperature in the tank. Feedback is the best method since the change of water temperature is a slow process and the disturbance from the surroundings is hard to predict and measure for use as the control reference. Figure 2.19 shows a block diagram using feedback method.

Control engineering is done with three different techniques; a Proportional(P), Integral(I) and a Differential(D) part.

Proportional term (P-control)
The proportional term is the most basic and simple method of controlling a system with control engineering. It uses the difference between the current and wanted state to determine the control factor. It gives a larger response effect when the difference is high. While a small difference will give a small response

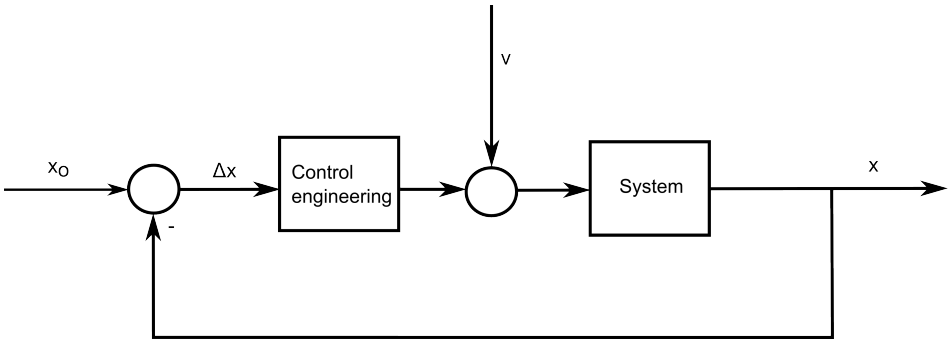

Figure 2.19: Block diagram of control engineering using feedback. x_0 is wanted state, x is current state and v is the disturbance on the system.

effect. This process can be shown in the block diagram in figure 2.19.

Integration term (I-control)
Using a P-controller alone is sometimes sufficient. However, the P-controller becomes inefficient when the system approaches the wanted state. This due to the small difference between current and wanted state which determines the effect of the P-controller. The integration term takes care of this problem. By integrating the difference over a given time window and multiply with the integration gain constant K_I. This is known as the integration term.

The integration term, makes the control engineering more efficient when the system is close to the set point. However, it may some time cause the system to oscillate around the set point. To prevent this is a damping function needed.

Derivative term (D-control) The derivative term has a damping effect on the changes in the system. It is used by calculating the slope of the changing state and multiplying it with a constant K_D. This is used to dampen the actuation on the system, e.g. the derivative term decrease the acting force on the system if the slope is high and is approaching the set point rapidly.

2.4.2 NI USB-6009 DAQ device

To control the temperature with a computer, a data acquisition device (DAQ) is needed. To do this a NI USB-6009 (fig. 2.20) is used. It reads signals as input and produces output signals. The DAQ device converts all input signals to digital signals before sending them, by a USB cable, to the computer. The NI

USB-6009 is crucial to operate the heating system, and is designed to work with the computer software LabVIEW (sec. 2.4.3). To control the ice tank 3 digital output ports and 7 analogue input ports are needed. For this the NI USB-6009 was a good choice. It had 8 single analogue inputs and 12 digital I/O channels [13].

Figure 2.20: Data acquisition device, NI USB-6009.

The NI USB-6009 is easy to configure and has high precision readings. It can read input signals from -10 to +10 V and produce voltage signals from -5 to +5 V.

2.4.3 LabVIEW

LabVIEW is a computer program based on graphical programming (G-programming) and is ideal for software development used for measuring and controlling systems. It contains all the functions engineers and scientist needs to perform a wide range of operations. It is built with focus to be developed efficiently by using the "drag and drop" principle.

LabVIEW is separated into 2 windows (see fig. 2.21), the front panel and the block diagram. The front panel is the window that the user will be operating when the program is running. This window contains buttons, boolean LEDs and plotting windows; tools needed for the operator to survey and operate the system/program.

The block diagram is where the actual programming is done. Here are all the functions, loops and statements declared. This window is only visible for the program developer. Function boxes are placed and connected using wires and all

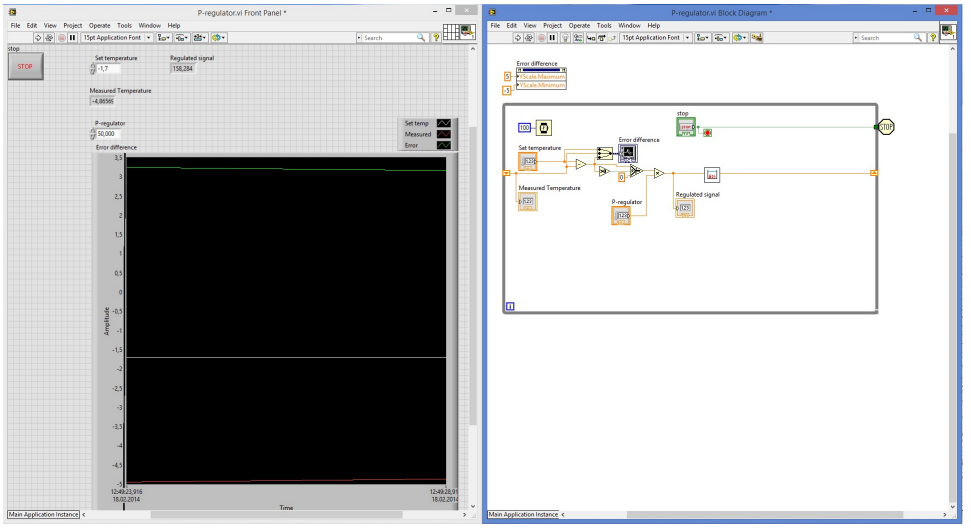

Figure 2.21: LabVIEW windows: The front panel(left), the block diagram(right).

information is sent between the functions through these wires. Loops are made by putting the syntax inside loop-frames, which indicates what is being looped.

2.4.4 LabVIEW program

When starting the development of the computer program a few basic goals were set. The program should be able to read user input, the temperature set point. It should also display the current temperature in the tank. During the process the need of more functions was discovered and the program continuously grew while programming. Features like overriding the heating cables and logging temperature. Also the possibility to determine which sensors should be used for temperature regulating was added.

The GUI was separated by a tab function; the "Main Window" (fig. 2.22a) and "Settings and Logging" (fig. 2.22b). The main window takes the user input "set temperature" and displays the current temperatures in the tank. The numerical displays of each sensor are located on a figure of the tank, placed at the sensors' actual position on the tank (fig. 2.8). This makes it easy to visualize the current temperature situation in the tank. Heating cable indicators are also located in this figure, together with the numeric temperature displays. They are boolean indicators which are lit when the heating cables are on. Also two indicators that are lit when the logging function is running and when the heating cables are

manually controlled are placed in the "Main Window" tab. This is because these functions should be turned off by the user before turning off the program, to prevent loss of logging data and to ensure the heating cables get turned off.

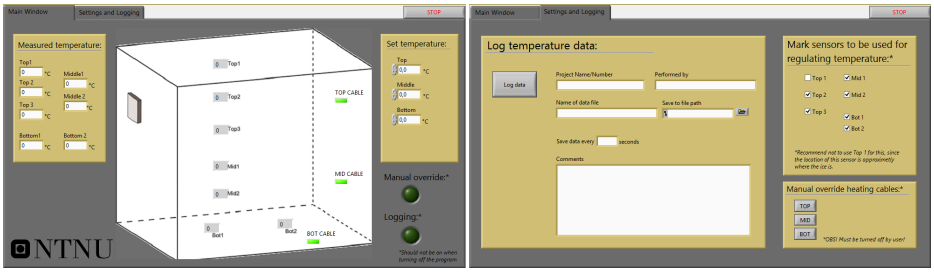

(a) First front panel LabVIEW program. (b) Second front panel LabVIEW program.

Figure 2.22: Graphic user interface of the LabVIEW program.

The "Settings and Logging" tab contains functions and settings the user may find useful. A logging function that creates a text file and saves all the temperature measurements together with the temperature set points for each section of the tank (Top, Middle and Bottom). The user decides how often the temperature should be logged in the text file by defining the sampling period in seconds. Together with the temperature data the user can save information about the experiment in the same text file ("name on project", "performed by" and additional comments).
The user may also choose what sensors should be used for temperature control, this is also a useful function in case a sensor should stop working. The average value of the measurements is used as input to the control engineering when more than one sensor is selected to control the heating system. This tab page also has a function that manually controls the heating cables. This is a practical function when removing ice from the tank.

The development of the block diagram was a long process and many modifications were done throughout the development. A simulation of the temperature changes in the tank was made since it was not possible to test the control engineering function directly on the tank from the beginning. This simulation was an estimate on how the temperature in the tank would change in reality. The results concluded that a PI-controller was needed when testing the control engineering on this simulation. Since tuning a PI-controller is a more demanding task, it was decided to perform the tuning of the PI-controller when connected to the

ice tank. It was discovered that the simulation of the ice tank was unrealistic when testing the finished controller on the ice tank, and it was sufficient with a P-controller. Changes were made and more about the calibration and tuning of the control engineering is found in section 2.5.3.

The signal control of the relays were done with inverted boolean signals. This means that when the heating cables was off a digital "true" signal was sent from the computer. The reason for this was that the relays needed a voltage potential difference of more than 3.5 V to be switched. The DAQ could not produce this voltage difference from the digital output and ground ports. Instead, the +5 V and digital signal output ports were used, and when the digital signal was set to low were the potential voltage difference larger than 3.5 V. Which was needed to switch the relay.

2.5 Calibration

2.5.1 Calibration methods

It is important to calibrate PRT sensors over a temperature range that represents the range of operation. There are two typical methods to calibrate PRT sensors; Fixed point calibration and comparison method.

Fixed point calibration is the most accurate method and uses the triple point (the temperature where solid, liquid and vapour state of an element occurs) of pure substances. This state is obtained by using specially built "cells" which can reproduce a substance's triple point. The sensor is calibrated by exposing it for this temperature and calibrate it to the known temperature of the triple point. The triple point of different substances is listed in The International Temperature Scale of 1990 [14]. The fixed point method is very expensive and its accuracy is often unnecessarily high for its application (0.0002 °C).

A well known fixed point calibration method is the ice bath, which is inexpensive and repeatable. Ice bath is made by mixing crushed fresh water ice with fresh water. An ice bath holds a temperature of 0 °C with an accuracy of ±0.1 °C, therefore is the ice-water relation very important. If the crushed ice is floating, the bath contains too much water which makes it unstable and the temperature may deviate from 0 °C. The preferable amount of water is 2/3 up in the crushed ice. The ice bath is a secondary method in fixed point calibration since it doesn't use triple points, which is the primary method.

Comparison method uses a highly accurate and known sensor as reference. By placing it together with the sensor(s) to be calibrated in a temperature stable environment the sensors are calibrated according to the reference sensor. This method is a faster, more efficient and cheaper than the fixed point method. Although the accuracy is lower (0.01 °C), depending on the accuracy of the reference sensor.

2.5.2 Calibration of sensors

A small deviation in measured temperature in some sensors was discovered after mounting the sensors to the tank. The observations resulted in the sensors needing calibration. Since the sensors already had been mounted on the tank, was a comparison-method calibration hard to perform due to the distance between the sensors and the difficulties in creating a temperature stable environment. A more executable method was the ice bath, which is the secondary fixed point

calibration method.

The calibration was performed by mixing fresh water ice and fresh water in a closed plastic bag. This bag was placed on the sensor's contact area on the tank's inside. The bag was held at this position until the sensor reading stopped declining, at this point was the measured resistance (eq. 2.3) over the sensor adjusted with a term ΔR until the measured temperature showed 0 °C. This resulted in the new temperature being calculated from equation 2.20.

$$R(T) = R_0 \left(1 + A \cdot T + B \cdot T^2\right) \underline{+ \Delta R} \tag{2.20}$$

The calibration showed that the sensors needed adjustment for measuring too low temperatures. They were adjusted maximum by 1.9 Ω, which translate to a temperature adjustment of approximately 0.47 °C.

2.5.3 Calibration and testing of computer program

After deciding to go for a P-controller, a calibration of the controller was needed. First off was the proportional gain set to be $K_P = 10$. The system was further on divided into 3 parts; when the control engineering output y>10 was full heating on, 0<y<10 was 50% on and when y=0 was zero heating on. The system was turned on and the logging function was set to log the temperature every 5th minute. After a few hours was the system turned off and the logged data was examined and plotted. The resulting plots are shown in figure 2.23-2.25.

As figure 2.23 shows, the set temperature was never achieved in the upper part of the tank. The data point for Top3 seems to stop at 0.2 °C below the set temperature. The data series for Top2 are much lower than Top3. This is caused by ice, and not water, covering the sensor area. Top1 sensor is not included in this test due to an error in the amplification circuit at that moment.

Figure 2.24 shows the temperature in the lower part of the tank was stable but never achieved the set point. Mid1 sensor was mostly at 1.8 °C and Mid2 at 1.7 °C. This is the same as the results from the upper part of the tank, where the measured temperature is 0.2 °C under the set temperature.

Figure 2.25 shows the same pattern as in figure 2.23 and 2.24, the measured temperature is approximately 0.2 °C below the set temperature. This shows that the regulating system needs to be adjusted. The reason must be that the disturbances from the surroundings are greater than expected and more heat is needed when approaching the set point.

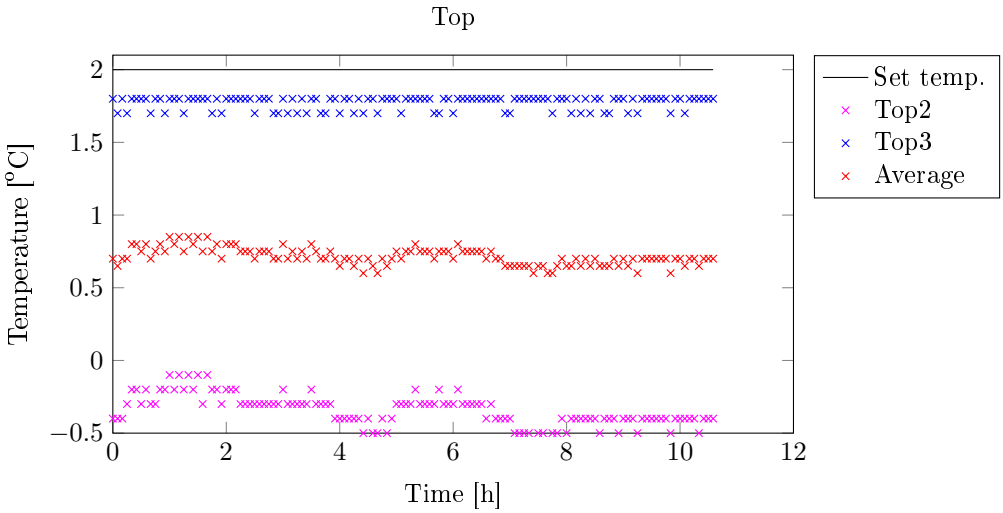

Figure 2.23: Plot of top section temperature before calibration.

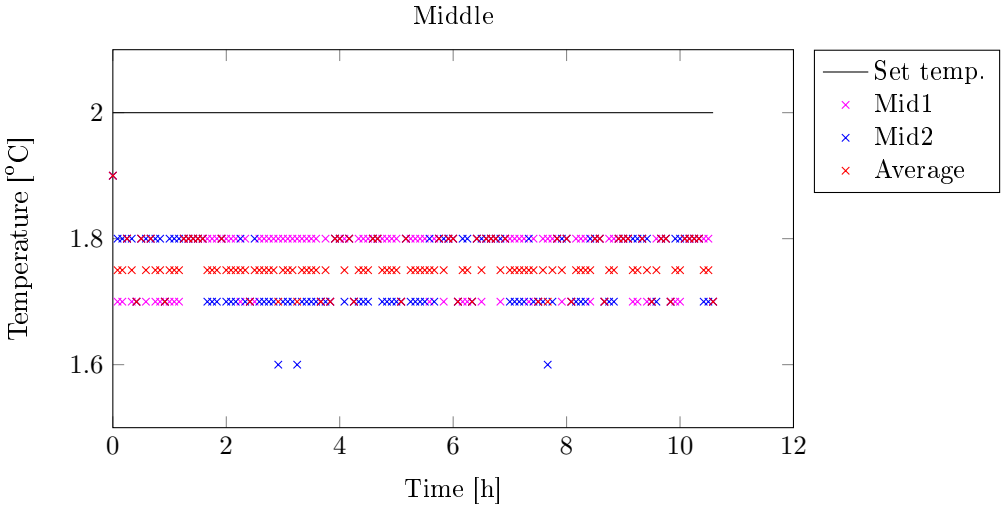

Figure 2.24: Plot of middle section temperature before calibration.

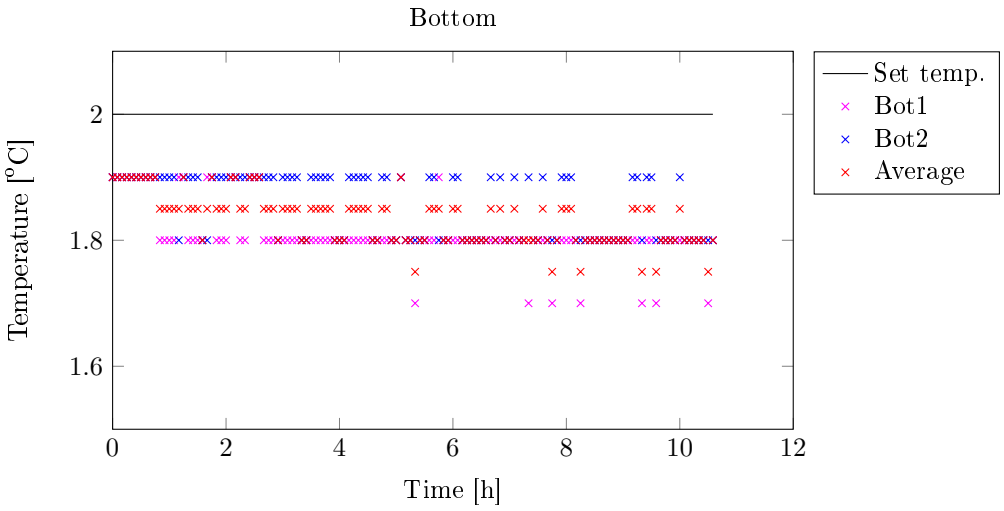

Figure 2.25: Plot of bottom temperature before calibration.

Final result

A final well functioning regulation was found after trying different settings through several days of testing and temperature logging in the tank. The reason for the calibration taking such a long time is due to the slow changes in the system. Temperature control is a slow process, and one test takes hours before any results can be used for a conclusion.

The final properties for the control engineering was divided into 5 steps. y>5 100% heating. 5>y>0 50% heating, y=0 5% heating and y<0 heating off. The 5% heating at y=0 is when the temperature has reached the set point. But to avoid a decrease in temperature, a small amount of heat is added. Approximately the same amount of energy leaving the system, and thereby making it stable. Figure 2.26 - 2.28 shows the temperature data from the last calibration test of the tank, where these properties was acting.

The temperature measurements are very good and only deviating from the set point by 0.1 °C, which might be caused by insufficient sensor calibration. In figure 2.26 is only Top3 sensor being used for temperature control. This because Top2 sensor was covered with ice, and Top1 sensor was affected by a hardware error, which later was fixed. The highest placed sensors Top1 is not recommended

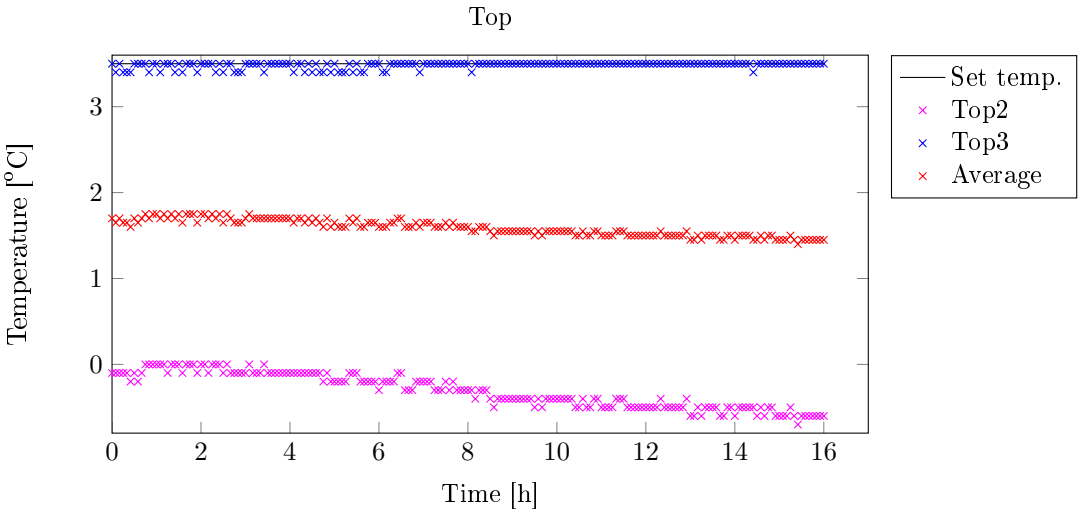

Figure 2.26: Plot of top section temperature after calibration, set temp.=3.5.

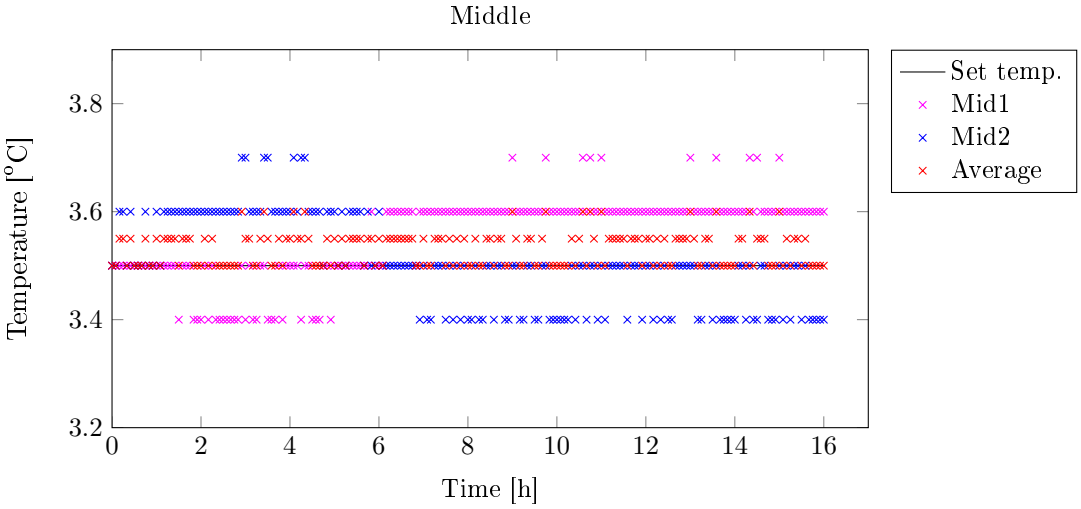

Figure 2.27: Plot of middle section temperature after calibration, set temp.=3.5.

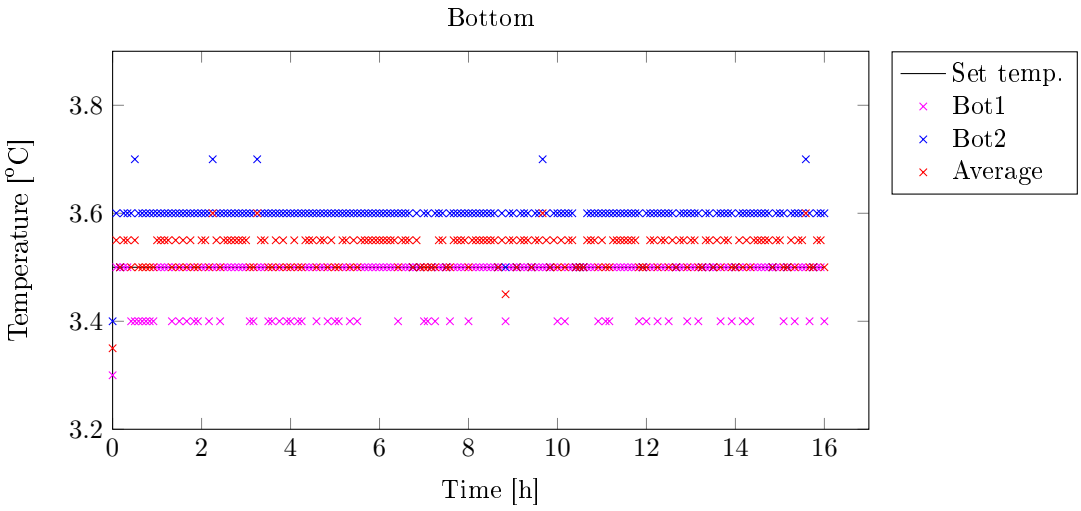

Figure 2.28: Plot of bottom temperature after calibration, set temp.=3.5.

to be used for temperature control since it is subjected to ice sheet coverage. It is primarily to be a part of the temperature profile and measuring ice temperature, when covered.

3 Testing and Validation

3.1 Sea ice structure

When water freezes, the molecules are arranged in a hexagonal structure. The solid state of water has a greater volume than the liquid state, resulting in ice floating.

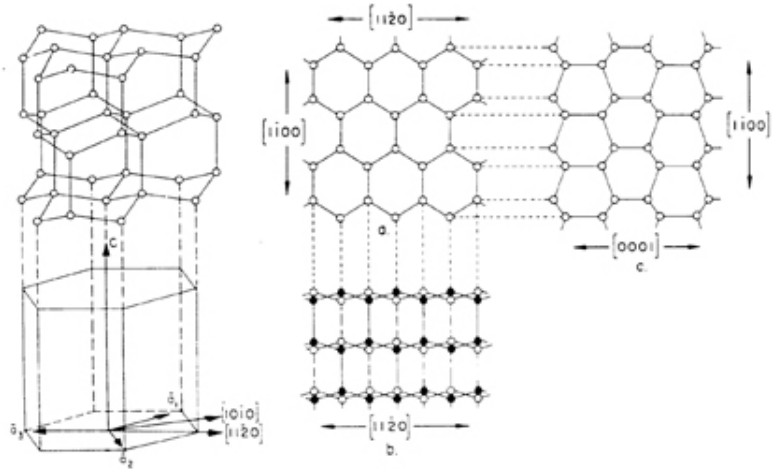

Figure 3.1: Structure of ice crystals of 1h ice [15].

The hexagonal ice structure constitutes a plane, called the basal plane and is illustrated in figure 3.1. The C-axis is a central term in the field of ice study. It is used to describe the orientation of ice crystals and is perpendicular to the basal plane. The C-axis, the optical axis, is shown in the left drawing in figure 3.1, inside the hexagonal structure.

The growth speed of sea ice is dependent on the heat transfer from the water through the ice sheet. As seen in figure 3.1 the molecules in an ice crystal are closer arranged in the basal plane, than in the direction of the C-axis. The close arrangement of molecules causes the heat transfer to go faster along this plane. This leads to ice growth development to be dependent on the orientation of the ice crystal. An ice crystal with a vertical basal plane will grow faster than a horizontal basal plane crystal.

In the first stage of ice growth, crystals are formed on the water surface and grows in the horizontal and vertical direction. The horizontal growth stops when there is no more room for the crystal in this direction. At this point the crystals starts to grow only in the vertical direction, and the orientation of the ice crystal is crucial for the continuing growth. Crystals with a horizontal basal plane will be encapsulated by more vertically oriented and faster growing crystals. This is called the transition zone, or wedge-out zone and is illustrated in figure **??**. The figure shows a horizontal basal-plane oriented crystal being encapsulated and out-grown by more vertical oriented crystals. Where the wedge-out zone occurs is strongly dependent on the conditions in the water, it can happens just below the surface or several decimetres down in the ice.

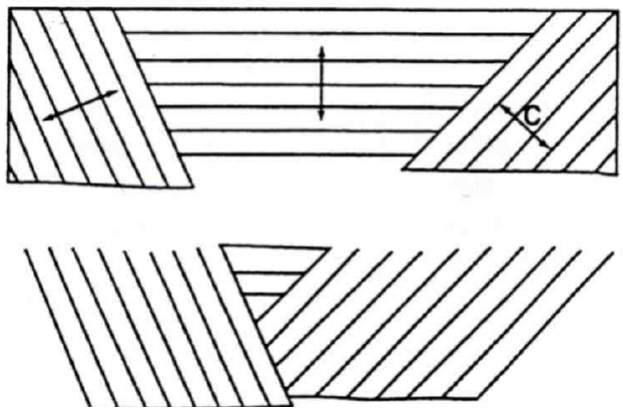

Figure 3.2: Illustration of wedge-out zone in ice growth. Lines indicates basal planes [16].

Sea ice consists mainly of two layers; the primary and secondary layer. The primary layer is the top layer of the ice sheet with the secondary layer located right underneath. These two layers are separated by the wedge-out zone.

Typical sea ice has a secondary layer called S2. An S2 ice consists of crystals which all have C-axes in the horizontal plane, but not necessarily in the same direction. This ice has a column structure in the vertical direction, meaning that the crystals grow parallel to each other creating "columns". This can be seen in figure 3.3.

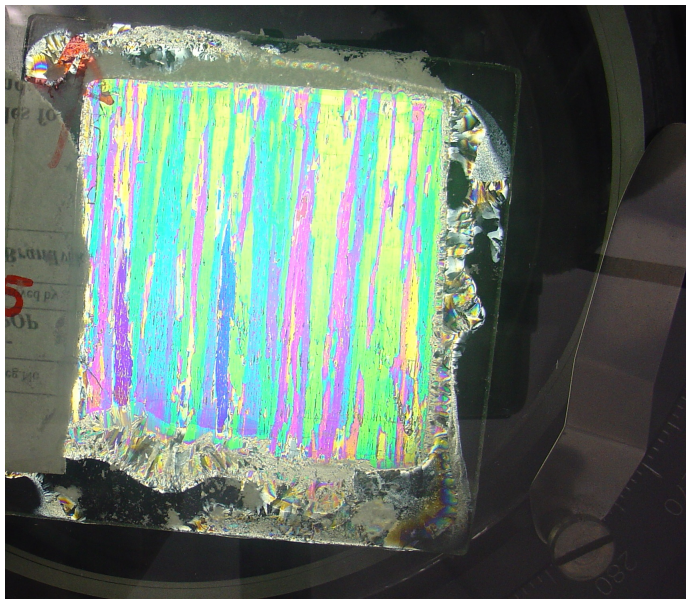

Figure 3.3: Thin section of S2 sea ice, showing columnar structure. Sample taken from land linked sea ice in Van Mijenfjorden on Svalbard.

3.2 Experiment procedure

3.2.1 Preparations

The tank is filled with water and the room temperature is set, usually to -20 °C. When sea ice is being made, salt is added while the tank is being filled. The amount of salt added to the tank is calculated based on the wanted salinity level. The salinity is given in ppt (parts per thousand) and is calculated as a mass relation with the water in the tank.

$$\begin{aligned} \sigma &= \frac{M_{salt}}{(M_{water} + M_{salt})} \\ &\Downarrow \\ M_{salt} &= \frac{M_{water} \cdot \sigma}{1 - \sigma} \end{aligned} \tag{3.1}$$

where M_{salt} and M_{water} is the mass of salt and water given in kg. σ is the wanted salinity level and is given as $\frac{ppt}{1000}$. It is important to stir properly so all salt is dissolved. Not doing this results in not achieving wanted salinity level.

Next step in the preparation is to turn on the heating system to keep the water above freezing point. The freezing temperature is calculated by using equation 3.2.

$$T = \frac{\sigma}{\alpha(1 - \sigma)} \tag{3.2}$$

where $\alpha = -0.0182$, σ is the water's salinity level given as $\frac{ppt}{1000}$ and T is the freezing point given in °C [17]. This expression only applies for freezing temperatures in the range $0 > T > -8.2$ °C. The heating system set point is set to be approximately 0.1 °C above the freezing point.

When the water in the tank is close to its freezing point any ice on the surface is removed and the water is stirred. When creating sea ice low salinity water is sprayed on the surface, landing on the surface as small crystals to initiate growth. This solution contains a lower level of salinity, usually half the level of the water in the tank, this to prevent it from melting when landing on the surface. The amount of salt to add to the spraying bottles is also calculated from equation 3.1. When the spraying is finished, the tank is covered by a wooden plate, leaving the ice to grow.

3.2.2 Thin sections

A thin section is a $\approx 0.3{-}0.5$ mm thick ice sheet that is made from a sample of sea- or fresh water ice. Thin sections are an important tool and is used to study grain

sizes and the structure of ice. By studying these properties can an assumption or determination of ice type (P1, S2, etc.) be made. Common thin sections to make are horizontal and vertical sections, relative to the ice sheet. Horizontal thin sections are made to study grain sizes and growth in the horizontal plane, while vertical thin section are made to study the ice structure development down through the ice.

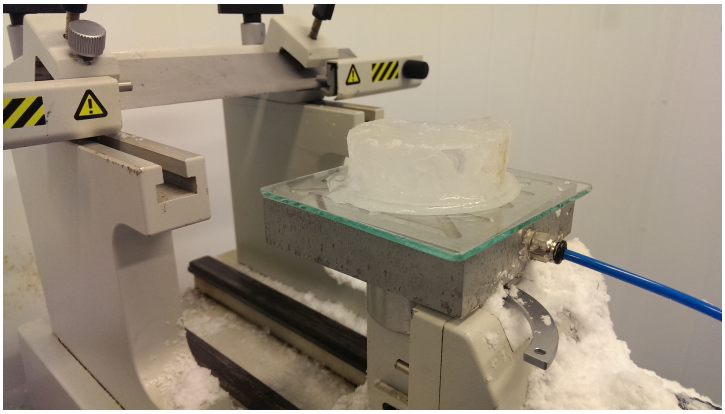

Figure 3.4: Ice sample glued to glass being planed by using a microtome to make a thin section.

Thin sections are made from cylindrical ice samples taken in the vertical direction of an ice sheet. Each sample can give 1-3 thin sections, dependent on the ice sheet thickness. The samples are cut by using a band saw, and each part's thickness is measured. This is done to track the depth position of the thin section. After measuring the thickness, the cut out sample is it glued to a 3mm thick glass plate by spurting fresh water around the edges. The glass plate is held fixed on the microtome by using suction from an air pump (blue tube) creating vacuum underneath the glass (see fig. 3.4). Then the sample is planed by sliding it back and forth under a knife, removing just a few micrometer by each slide. When the sample is smooth and free of bubbles, it is turned so it can be planed on the other side. First the remaining sample thickness is measured to know how much ice has been planed off. Then the planed side is glued to a new glass plate. Now the sample is glued between two glass plates. The first plate is then removed by using a band saw. The glass with the planed sample side is now placed on the microtome and is planed to a finished thin section of approximately 0.3-0.5 mm thickness. The finished thin section is now ready to be examined. Merely looking at the thin section in normal light would not give much information about the grains and structure. Figure 3.5 shows a picture of a thin section lit by white

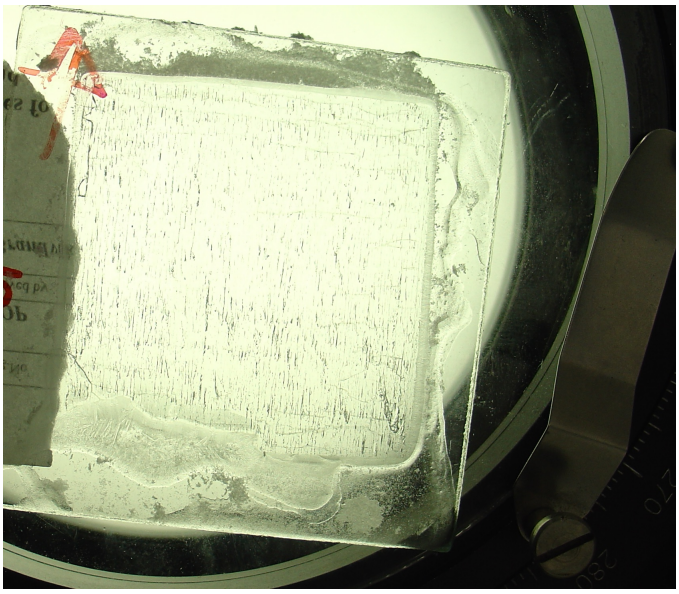

Figure 3.5: Vertical thin section held above white light.

light. But if the thin section is studied through a polarization filter then much more information revealed (see fig. 3.3 and 3.6).

Each colour in figure 3.3 are individual grains. This means that in this thin section the crystals are growing vertically (from top to bottom). The reason that colours appear when examined through a polarization filter is because of the orientation of the ice crystals, affecting the light propagation through the millimetre thick ice. Light gets dispersed when it propagates through the crystal, due to optical effects. The dispersed light propagates up to the polarization filter where the light gets polarized resulting in only one colour reaching the eye. Since the light dispersion is dependent on the crystal orientation, do all grains with the same colour have the same crystal orientation (direction of C-axis).

The red border in figure 3.6 marks one crystal grain seen in a thin section. The grains in figure 3.6 are growing downwards giving columnar ice. Columnar ice might also grow in the horizontal direction, but that is not characterized as S2 ice.

The process of making a thin section takes time and patience. If not careful, the thin section may break before getting thin enough, and the results are lost.

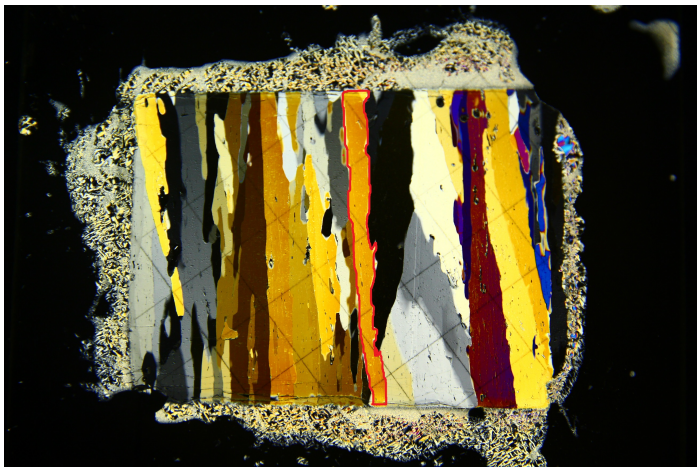

Figure 3.6: Marked grain seen in a thin section.

A good way to avoid loss of result is taking pictures of the thin section before reaching the wanted thickness in case it breaks, then at least some results are recorded.

3.3 Fresh water ice experiment

The first experiment conducted in the tank after the modifications was a fresh water ice experiment. It was conducted together with Nicolai Greaker, another master student working in the cold lab. The results were interesting and useful as validation due to this being the first experiment after the modifications. Properties being examined were thickness along the walls (ice profile along the water surface) and the temperature control of the heating system.

Additional data and results from this, and all other experiments, are listed in the appendix A.

3.3.1 Method

The tank was filled with fresh water, the heating system was set to 0 °C and the growth period was 7 days in a room temperature of -10 °C.

3.3.2 Results

The ice sheet had a thickness of approximately 19 cm. An ice block showing the ice profile was cut out and is depicted in figure 3.7. The profile is perpendicular to the tank wall to see if any larger ice growth at the walls had occurred. The picture in figure 3.7 shows that there is no significant larger growth along the tank wall, compared with parts of the ice sheet closer to the middle.

It was observed during sampling that the ice was very hard and difficult to cut. Also a high water pressure had built up under the ice during the growth, resulting in a large amount of water coming up when the first hole was made.

The temperature development in the tank during the ice growth was logged and is plotted in figure 3.8-3.10. The plot in figure 3.8 shows that the water temperature decreased linearly from the point the tank was filled until the set point was reached. Top2 sensor reached the freezing point before Top3 sensor, resulting in the heating system being turned on, preventing Top3 to reach 0 °C. Top1 was not included in this experiment. The plot in figure 3.9 shows the same linear pattern as in figure 3.8. In this plot, the temperature is stable at approximately $0 - 0.05$ °C. The plot of the temperature development in the bottom of the tank shows that the temperature never reached the set point of the heating system, leading to the heating cables never being turned on.

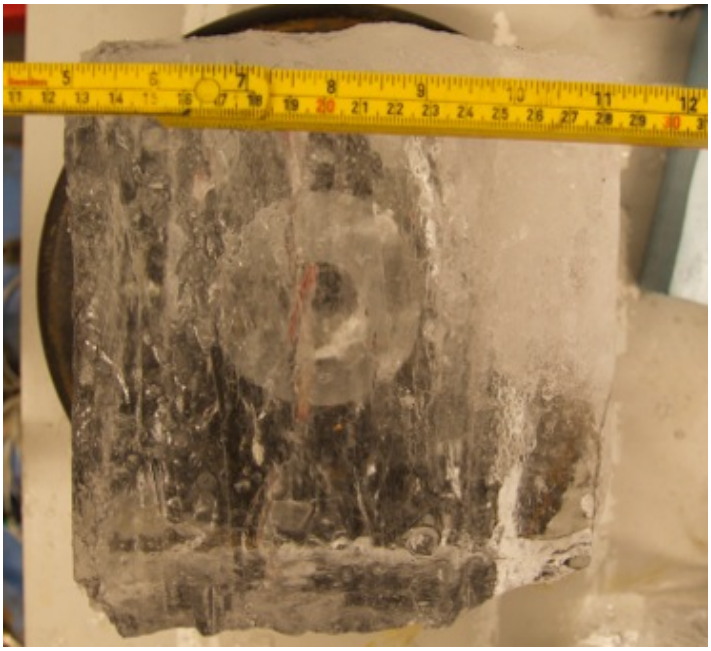

Figure 3.7: Fresh water ice growth profile along the tank wall. Orientation: tank wall along the left side of the ice block and bottom of the block is the bottom of the ice sheet (Photo by: Nicolai Greaker).

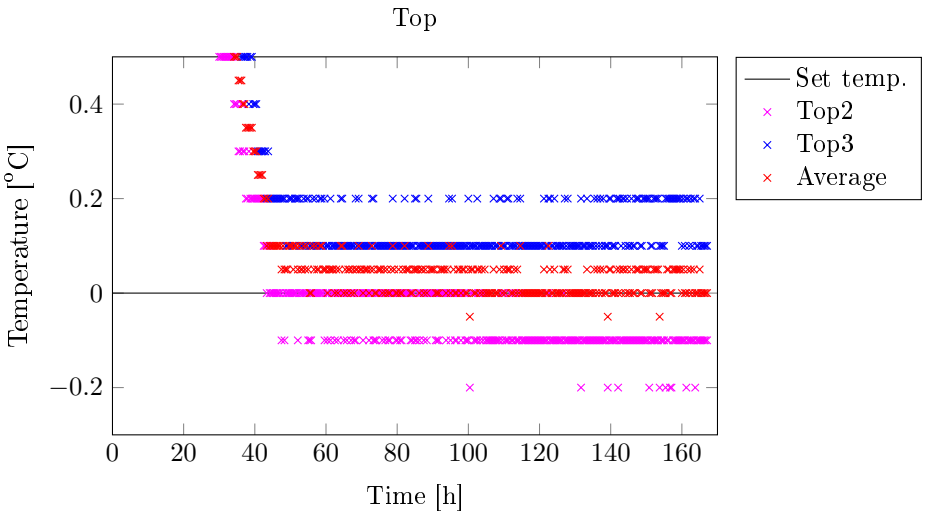

Figure 3.8: Plot of measured temperature in top section during fresh water ice growth.

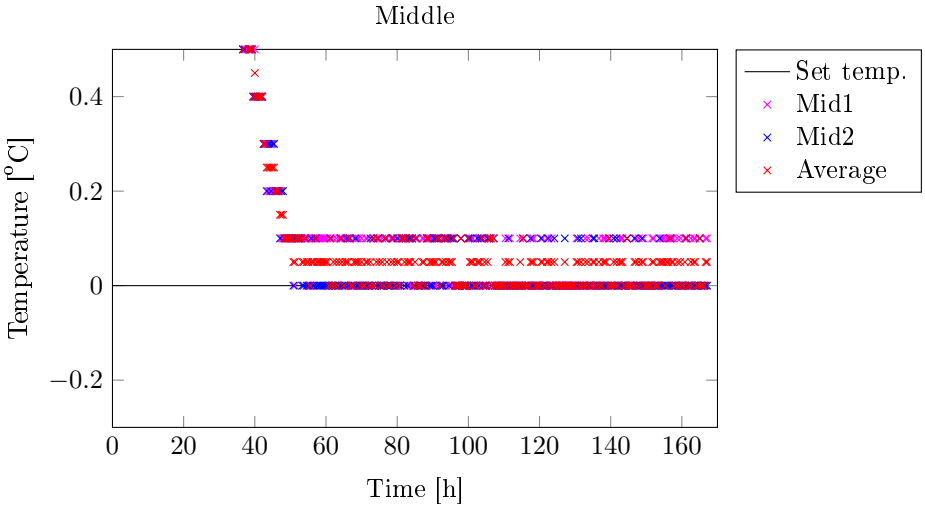

Figure 3.9: Plot of measured temperature in middle section during fresh water ice growth.

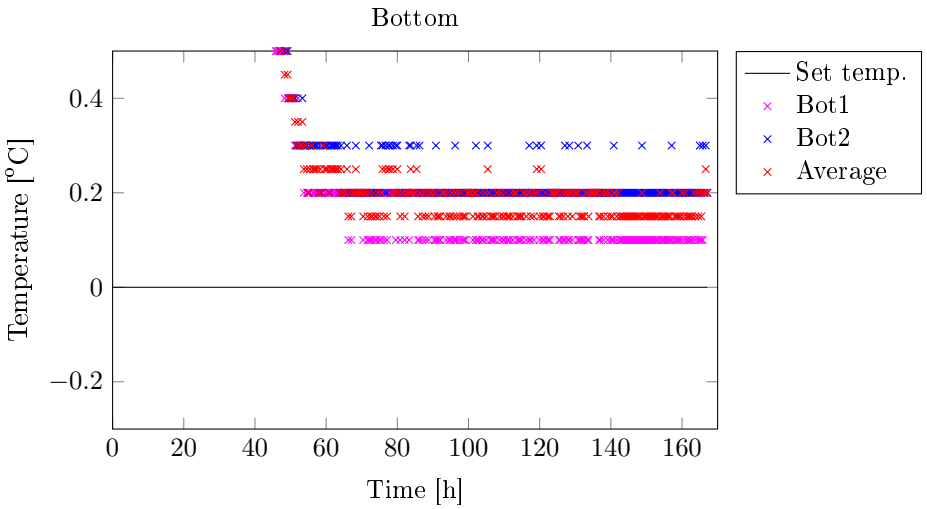

Figure 3.10: Plot of measured temperature in bottom section during fresh water ice growth.

3.4 Motivation to look at the spraying technique

From the project assignment *"Properties and growth of laboratory made columnar saline ice"* [1] were different techniques to produce sea ice in cold lab tested. Two methods were tested, resulting in four different combinations.

- Spraying
- Stirring
- Spraying and stirring
- Neither spraying nor stirring

The results showed that the combination of spraying and stirring gave the best outcome. The test consisting of spraying only, also contained good results, but this was not consistent over the whole ice sheet. However, another discovery from these two tests was made; The size of the column ice crystals from the spraying test were significantly smaller than the crystals from the stirring and spraying test. The reasons for this result were discussed in the report, and a possible reason could be the time spent on the spraying event. The spraying and stirring test was done over a significantly longer time window than the spraying test. This gives the hypothesis:

Does the time used on the spraying event affect the size of the ice crystals?.

The next two experiments will test if the spraying time will affect the size of the crystals in the ice sheet. The water will be stirred in both tests, so a constant temperature in the whole tank in the start is assumed.

The two test to be done are:

- Spray low saline water solution on surface over a time window of 15-20 min
- Spray low saline water solution as fast as possible

3.5 Sea ice experiment 1: Long spraying time

3.5.1 Method

The first sea ice experiment was to look at how the ice crystals developed when the spraying was conducted over a long time window. Also investigating whether the ice thickness was constant over the whole ice sheet, temperature development and if columnar ice occurred along the walls.

The desired water salinity level was 8 ppt. The water volume was 120x80x115 cm^3 resulting in adding 8.2 kg of salt, according to equation 3.1. The measured salinity level after mixing was 8.3 ppt. Water with a salinity level of 8.3 ppt has a freezing point at -0.46 °C (eq. 3.2). The heating system set point was set to -0.3 °C (approximately 0.1 °C above the freezing point) and the room temperature was set to -20 °C. The cooling process of the water took approximately 2 days.

During the cooling process thin ice layers were created on the surface. These were regularly removed until the water reached -0.2 °C and spraying could be conducted. Three 0.7 L bottles of 4 ppt (2.8 g salt) saline water was sprayed over the surface. The spraying process lasted 16 minutes and 40 seconds.

After five days the water temperature under the ice was control measured with a temperature gauge. It was measured to -0.3 °C while the ice thickness was measured to 8.5 cm. This was a unexpectedly slow growth, so the heating system set point was adjusted to -0.4 °C. The ice was removed three days later, after a growth process of totally 8 days.

3.5.2 Results

Temperature control

Figure 3.11 shows the temperature development in the upper part of the tank during the growth period. The heating system used sensor Top2 and Top3 to control the temperature. As the plot shows, the average temperature is 0.05 °C above the set point due to Top3 mostly being 0.1 °C above the set point. The water temperature changed quickly after the heating system set point was adjusted to -0.4 °C. Top1 sensor measured lower temperatures already after 20 hours of growth. The measured temperature in Top1 dropped slowly down to -1 °C during the 200 growth hours. After approximately 210 hours did the measured temperature in Top2 and Top3 drop by ≈ 0.4 °C. This was caused by a power shut down in the lab due to a fire in the neighbouring lab.

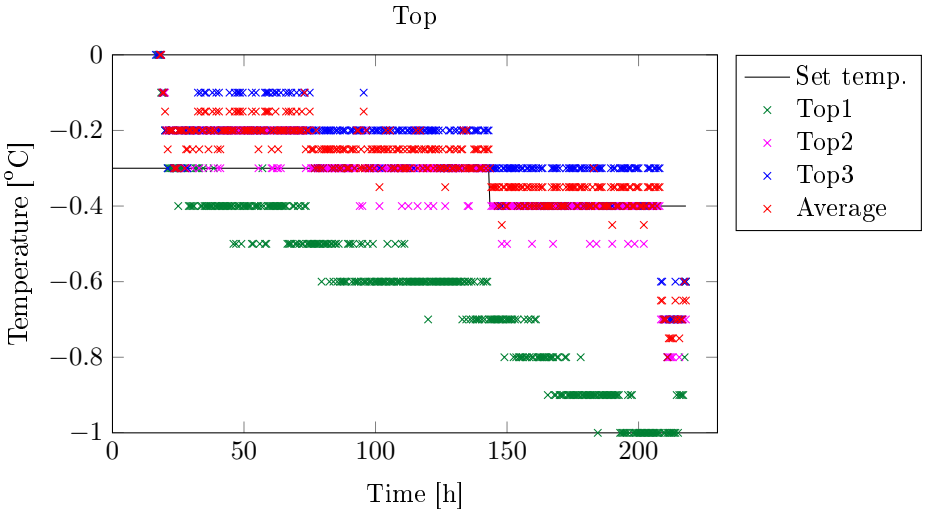

Figure 3.11: Plot of measured temperature in top section during ice growth of sea ice experiment 1.

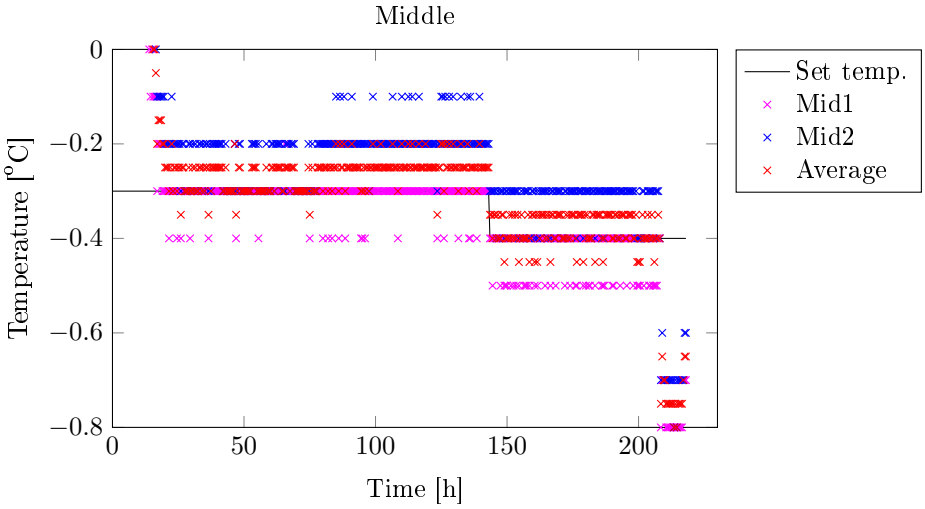

Figure 3.12: Plot of measured temperature in middle section during ice growth of sea ice experiment 1.

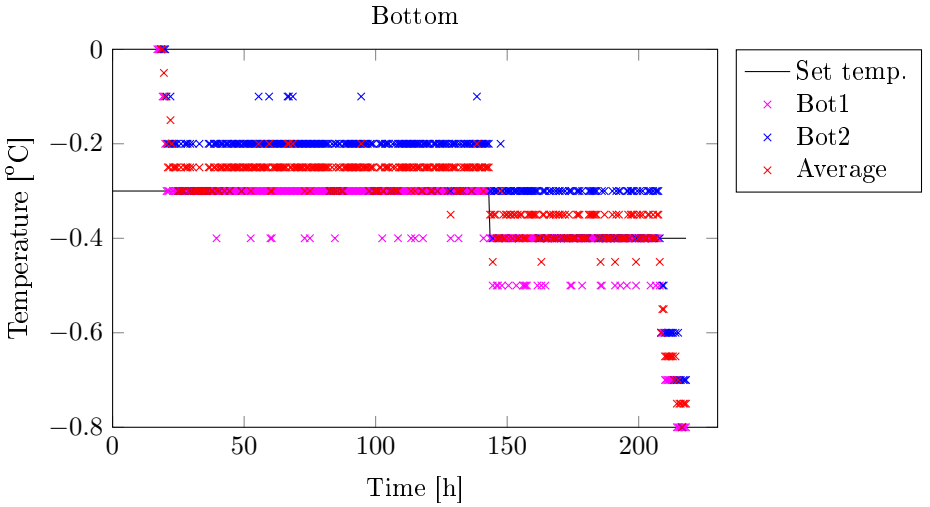

Figure 3.13: Plot of measured temperature in the tank bottom during ice growth of sea ice experiment 1.

Figure 3.12 shows the plot of the temperature development in the lower part of the water tank. The same pattern is seen here as in figure 3.11. The measured temperature in one of the sensors is mostly 0.1 °C above the set point making the average temperature being 0.05 °C above the set point temperature. Also in the lower part of the tank did the temperature change right after the adjustment of the set point temperature. The temperature in the lower part of the tank did also drop by 0.4 °C when the power was turned off.

The temperature situation in the tank bottom during the ice growth is plotted in figure 3.13. Bot2 sensor measured a temperature 0.1 °C above the set point resulting in the average temperature being 0.05 °C above set point. This means the bottom heating cable only was turned on when Bot2 sensor measured the set point temperature, resulting in the temperature at Bot2 shifting between −0.2 ° and −0.3 °C during the whole growth period. Also the bottom temperature in the tank dropped by 0.4 °C when the power was turned off.

Thin sections

Figure 3.14 shows a horizontal thin section at the top layer just 9.8 mm under the ice surface. The grain sizes is of approximately $3 - 5$ mm in diameter. The

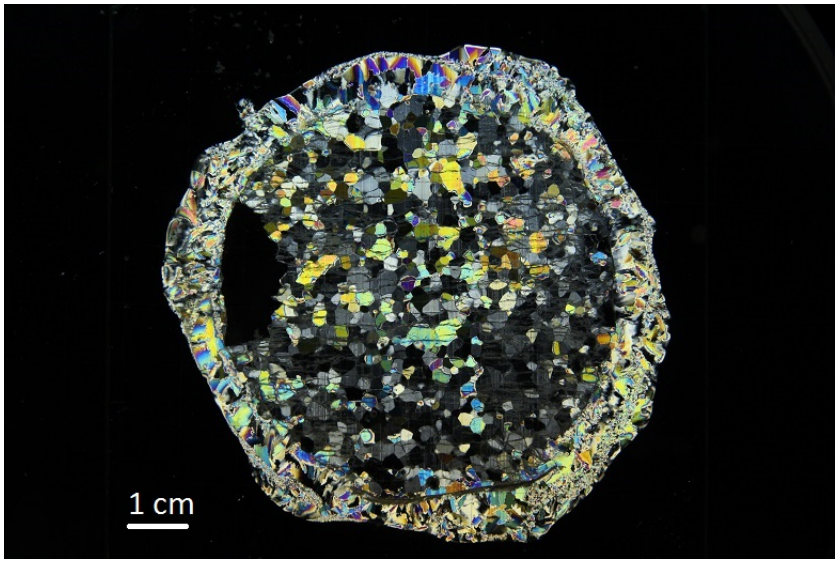

Figure 3.14: Top horizontal thin section, middle of ice sheet (9.8 mm below surface).

relatively large appearance of black grains indicates a common crystal orientation in the ice sheet. A horizontal thin section from the bottom of the ice sheet center is depicted in figure 3.15. It is hard to determine crystal sizes, due to many of crystals having the same orientation. However, the width seems to range from just a few millimetres to 1 cm. A vertical thin section from the center of the ice sheet is shown in figure 3.16. The thin section is a whole sample since the ice sheet was less than 10 cm thick in the middle. It is clearly visible that the wedge-out zone occurred approximately 2 cm down in the ice. After the wedge-out zone is columnar ice seen with a column width of $1 - 6$ mm. The black areas in the thin section is caused by the ice being planed completely off by the microtome.

A vertical thin section was done perpendicularly on the tank wall and is depicted in figure 3.17, with the wall located to the right of the thin section. There are clear indications of columnar ice with crystals oriented in different directions. The crystals are not growing completely vertically, but have a slope towards the tank wall. The wedge-out zone can be seen 1.5 cm down in the thin section.

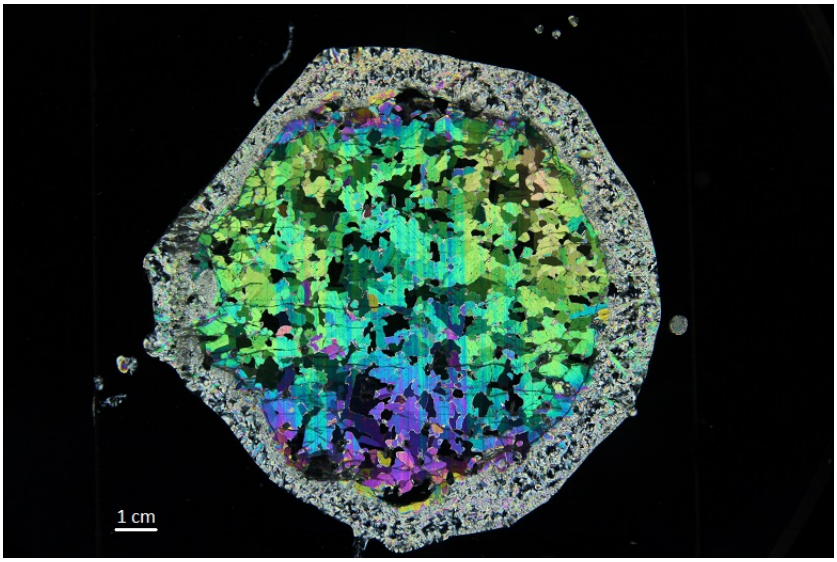

Figure 3.15: Bottom horizontal thin section, in the middle of the ice sheet (54.9 mm below surface).

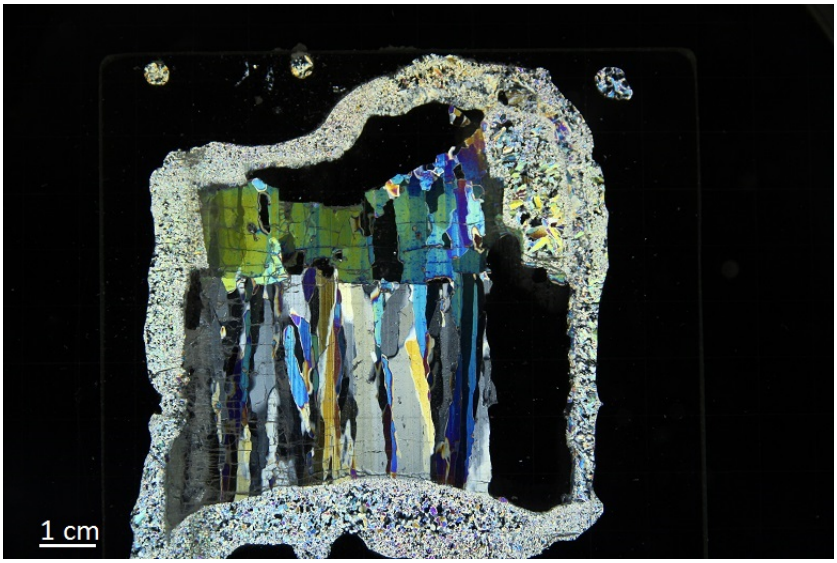

Figure 3.16: Vertical thin section, in the middle of the ice sheet (whole sample, 80mm).

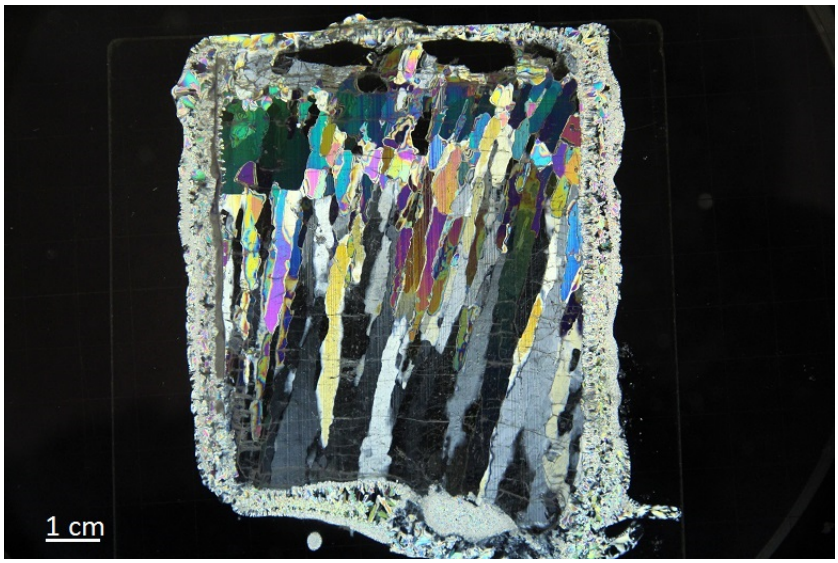

Figure 3.17: Vertical thin section, perpendicular to the tank wall (whole sample, 80-100mm), wall to the right.

Ice thickness

An ice block was cut out from the ice sheet along all four tank walls and is depicted in figure 3.18a-3.18d. As the figures show, the ice sheet was not evenly horizontal along the water surface, but thicker along the walls. However the thickness decreased rapidly from the walls and towards the middle. An approximation of the decreasing angle is given for each ice block in figure 3.18a-3.18d. A difference in thickness between the walls was also discovered. The ice thickness along the walls were thickest by the left wall (≈ 17 cm) and thinnest by the front wall (≈ 10 cm). Also the left wall ice block showed a faster growth in the corner between the back wall compared with the front wall corner.

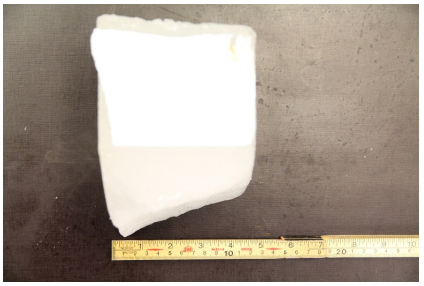

(a) Left wall. Angle ≈ 19 °.

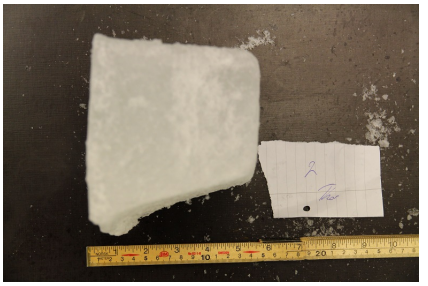

(b) Front wall. Angle ≈ 18 °.

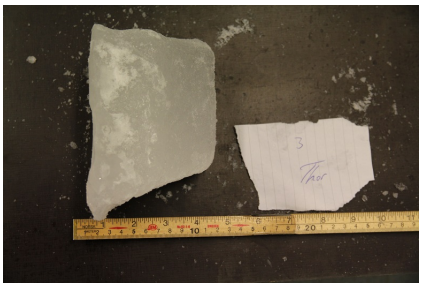

(c) Right wall. Angle ≈ 22 °.

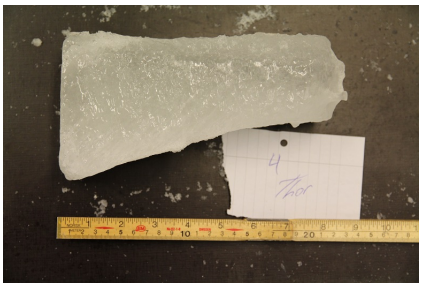

(d) Back wall. Angle ≈ 18 °.

Figure 3.18: Ice blocks showing thickness along each tank wall.

By using the data from each sample taken from this ice sheet, is the thickness plotted in figure 3.19. Each blue circle is a data point used to make an interpolation of the ice sheet thickness. The plot shows that the ice located more than 20 cm from the walls has a relatively constant thickness. The front right corner is not plotted because no samples were taken at this location.

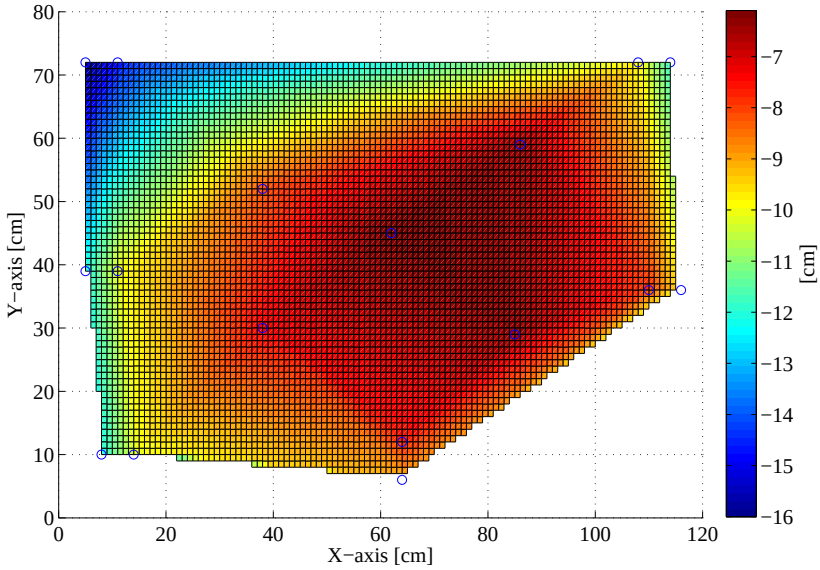

Figure 3.19: Contour plot of ice sheet thickness from experiment 1. Seen from above with axes representing tank boundaries. Back wall(y=80), Front wall(y=0).

3.6 Sea ice experiment 2: Short spraying time

3.6.1 Method and data

With the second sea ice experiment, the same properties were examined (thickness, temperature- and crystal development). But in this experiment, the spraying sequence was preformed in the shortest time window possible. Also for this test, the new wooden panels were installed, a voltage loss in the signal cable was fixed resulting in the sensors needed to be recalibrated.

Since this experiment was being compared to sea ice experiment 1, similar tank conditions were created. The salinity level was measured to 8.3 ppt and the heating system set point was set to -0.3 °C. The room temperature was set to -20 °C.

Thin ice layers occurred at the water surface during the water cooling period. When the water temperature reached -0.2 °C all ice was removed and the stirred to create a homogeneous temperature state in the tank. After this, spraying was performed in a time window of 9 minutes and 15 seconds. The spraying solution was of the same amount and salinity level as in the previous experiment (3x0.7 L of 4 ppt). A top cover was placed over the tank with a 20 mm thick polystyrene covering the left part of the surface. This was done as a test to try to prevent the larger ice growth along the walls on the left side, which had occurred in previous experiment.

After five days the ice thickness was measured to 5 cm. Due to this slow growth the heating system set point was changed to -0.4 °C. The ice was removed after 13 days of growth.

3.6.2 Results

Temperature control

Figure 3.20 shows a plot of the temperature development in the upper part of the tank during the growth period. Top1 shows lower temperature measurements than Top2 and Top3. After 3 days in the growth period, Top1 starts to measure decreasing temperature, which continues to decrease linearly down to -1.3 °C during the 13 days growth period. Top2 and Top3 are held constantly around the set temperature. Top2 shifts between the set point and 0.1 °C above, though the average temperature is mostly on the set point. It seems like Top2 stabilises at the set point in the end of the growth period. Figure 3.21 shows a plot of the temperatures measured in the lower part of the tank during ice production. Mid2

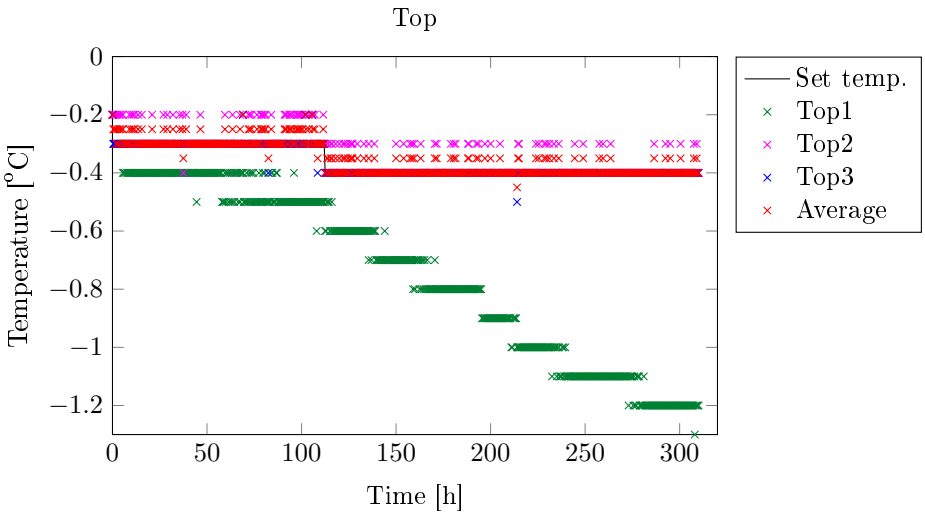

Figure 3.20: Plot of measured temperature in upper section during ice growth of sea ice experiment 2. Set temperature changes from -0.3 ° to -0.4 °C after ≈ 110 hours.

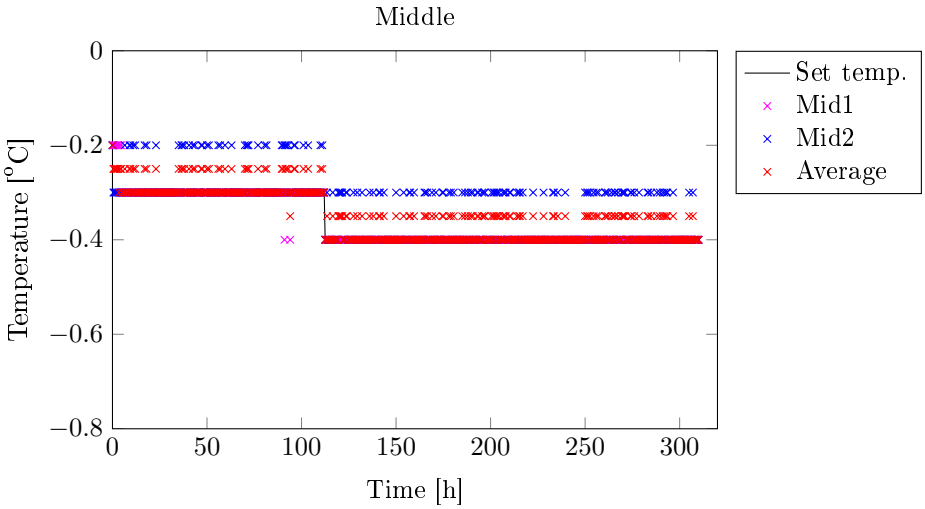

Figure 3.21: Plot of measured temperature in lower section during ice growth of sea ice experiment 2. Set temperature point changes from -0.3 ° to -0.4 °C after ≈ 110 hours.

sensor switches between -0.3 ° to -0.4 °C, causing the average temperature to be 0.05 °C above or at set point.

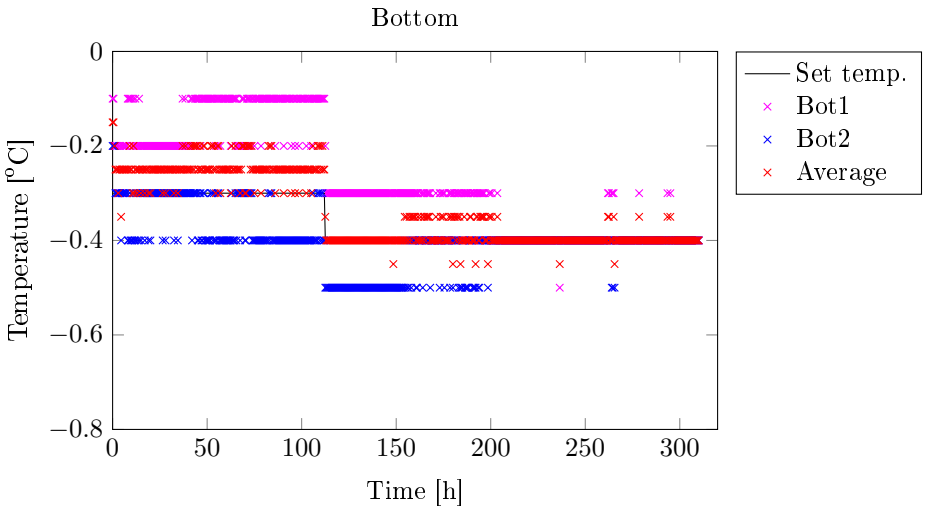

Figure 3.22: Plot of measured temperature in tank bottom during ice growth of sea ice experiment 2. Set point temperature changes from -0.3 ° to -0.4 °C after ≈ 110 hours.

The plot in figure 3.22 shows that the temperature varied from -0.4 ° to -0.1 °C during first 100 hours of the ice production. During this period the average temperature never got down to the set temperature, resulting in the bottom heating cables never being switched on. When the set point is changed after 110 hours, the average temperature is at set point the rest of the growth period and both sensors, Bot1 and Bot2, are stabilised.

Thin sections

A vertical thin section from the middle of the ice sheet is depicted in figure 3.23. It is clear that the wedge-out zone has occurred early in the process, less than 10 mm down in the ice. A large amount of columnar ice can be seen in the first centimetre of the thin section, having a width of $1 - 3$ mm. But when the ice reached a thickness of approximately 3 cm the columnar ice crystals were interrupted and stopped by large horizontal crystals. The colours do not indicate any common crystal orientation.

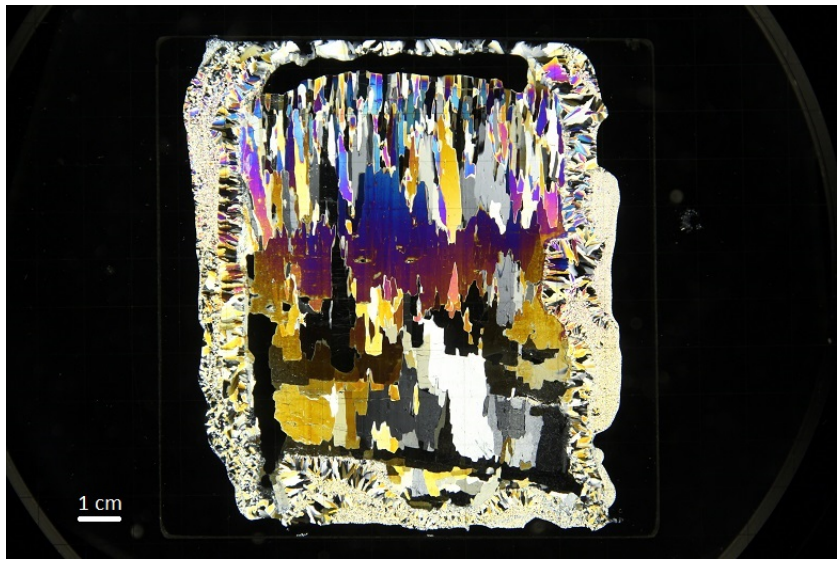

Figure 3.23: Vertical thin section, middle, whole sample.

Figure 3.24 contains a picture of a horizontal thin section located 10.5 mm down in the ice. The large amount of blue coloured grains indicates many of the crystals are oriented in the same direction. The size of the grains are from less than 1 mm to approximately 3-4 mm.

The grain width in the horizontal thin section in figure 3.25 ranges from 1 to 3 cm. Some parts of the thin section is black due ice having fallen off during planing. However, it is possible to see an indication of crystal alignment in the left part of the figure. The crystals seems to align in a 70° angle towards left.

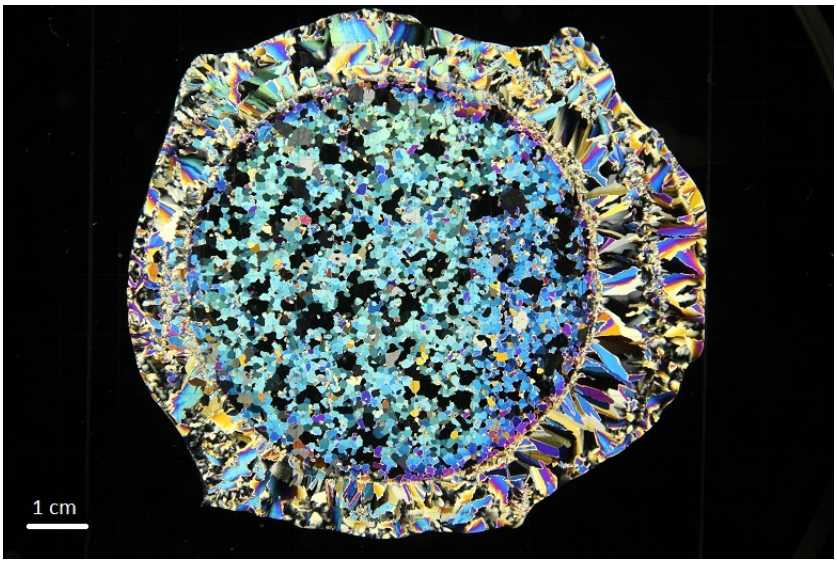

Figure 3.24: Top horizontal thin section, middle, 10.5 mm down.

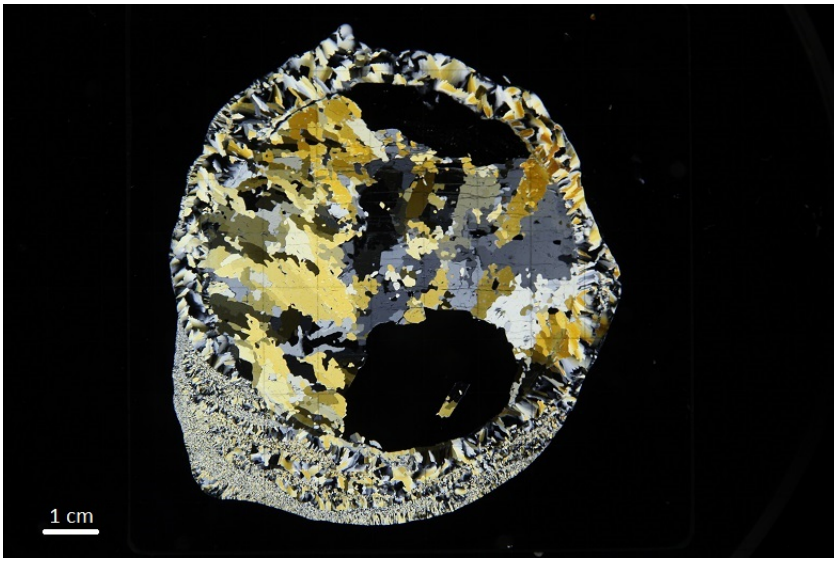

Figure 3.25: Bottom horizontal thin section, middle, 97 mm deep.

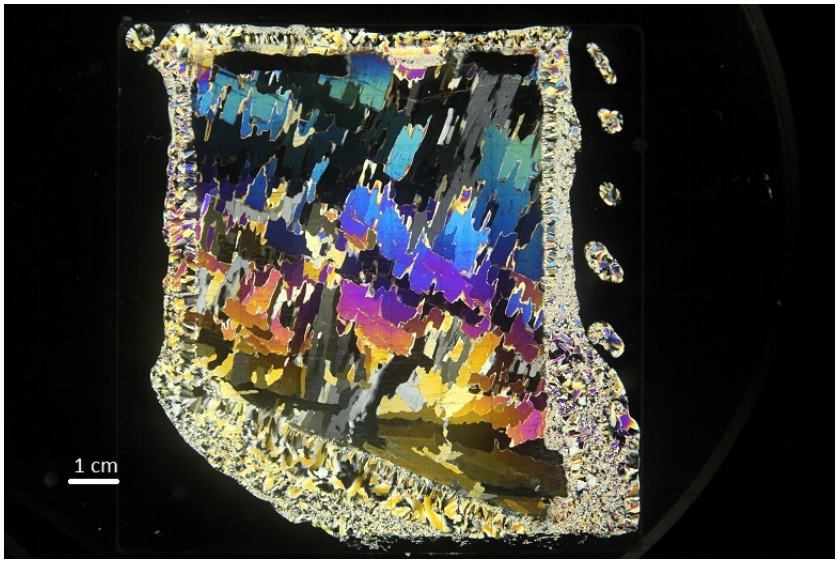

Figure 3.26: Vertical thin section along wall. The top is 42 mm below surface.

Thin section were made close and perpendicular to the walls, one is depicted in figure 3.26. The droplets seen on the right side of the thin section indicates the direction towards the wall while the lower part of the thin section is the bottom of the ice. The thin section shows that there is a common crystal growth direction perpendicularly to the skewed ice bottom. There is no consistent presence of columnar ice, but some can be seen in the upper part of the thin section.

Ice thickness

Ice blocks along each tank wall were cut out, measured and photographed (fig. 3.27). The pictures show the ice sheet bottom was not horizontal. The ice had grown thicker along the walls compared with the center of the ice sheet. The thickness along the walls also varied between the different walls. The angles of slope underneath the blocks are listed together with ice thickness by the wall in figure 3.27a-3.27d. From this it seems the ice at the front wall underwent the largest change in thickness when moving away from the wall. A small skewness along the left and right wall was also detected. The ice blocks became thicker when approaching the left and right back corner.

(a) Left wall. Angle$\approx 11°$. 20 cm thick.

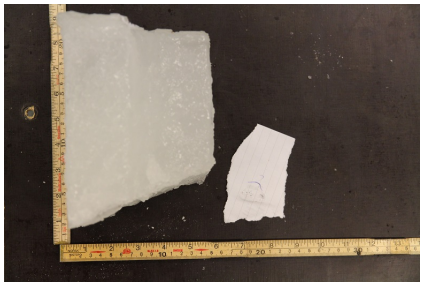

(b) Front wall. Angle$\approx 21°$. 17 cm thick.

(c) Right wall. Angle$\approx 17°$. 21 cm thick.

(d) Back wall. Angle$\approx 14°$. 19 cm thick.

Figure 3.27: Ice blocks from tank walls in sea ice experiment 2.

The measurements from the samples taken from the ice is used to interpolate a contour plot of how the ice thickness is distributed over the tank area. This plot is shown in figure 3.28. There is no data to do a interpolation of the ice thickness in the right front corner since no samples were taken in this area. It is clear that the ice is thicker along the walls and the thickest point is in the right back corner ($>$22 cm), by studying the plot. The parts of the ice sheet that is further than 20 cm from the walls has a more stable thickness all over. The blue circles in the

plot indicate the data points from the samples taken from the ice.

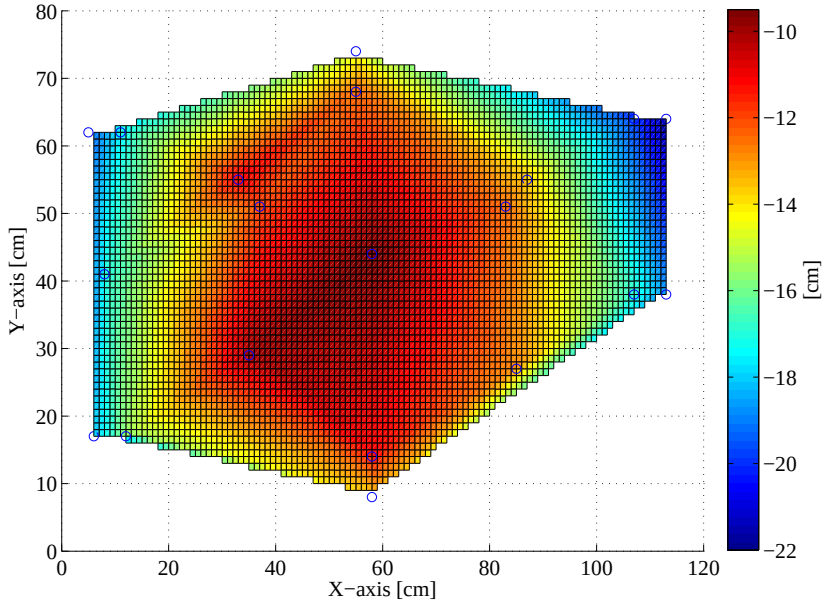

Figure 3.28: Contour plot of ice sheet thickness from sea ice experiment 2. Seen from above with axes representing tank boundaries. Back wall(y=80), Front wall(y=0).

4 Discussion

4.1 Measured temperatures and sensor readings

Three different experiments has been performed to test the new heating system. The upper part of the tank had three PT1000 sensors mounted and the resulting measurements from the tests is shown in figure 3.8, 3.11 and 3.20. Top1 sensor was not used in the freshwater ice test (fig.3.8) due to a hardware error .

The results from sea ice experiment 1 and 2 show that Top1 starts to linearly decrease in measured temperature before 20 growth hours have passed, while Top2 and Top3 are stable. This is explained by the location of sensor Top1. It is located 22 cm below the tank edge which is high enough for it to be covered by ice during growth. Top1 measures temperatures 0.8 °C below the set point temperature as seen in figure 3.11 and 3.20. The linear temperature decrease is caused by the ice getting thicker, and Top1's distance to the water increases. These measurements show that ice temperature gets lower by the surface as the ice thickness increases. This also shows that sensor Top1 can not be used in the control engineering of the heating system, but more as monitoring the ice temperature. This was the intention when the sensors were mounted.

Top 2 and 3 are approximately stable around the given set point (see fig. 3.8, 3.11 and 3.20). Top2 is oscillating between the set point and 0.1 °C above in the last two experiments, making the average temperature sometimes being 0.05 °C above the set point. This leads to the heating cables switching off each time the average temperature is above the set point and waits until the water is cooled down again. This occurred in every section of the tank in all the experiments), except in the bottom section in the freshwater ice test. The reason for measuring different temperatures in the same section might be caused by convective mixing. Convective mixing happens when there is local temperature difference in the water. Cold water sinks and is replaced by warmer water due to water density being

temperature dependent. The density peak of water is 4 °C for freshwater. This peak moves down in temperature with increasing salinity level, until the salinity level reaches 24.7 ppt. At this point water freezes before reaching its maximum density. Convective mixing stabilizes when all water temperature is lower than the density peak temperature. This does not apply when sea ice begins to form at the surface. When sea ice grows, it excretes salt and creates small pockets with high salinity water, called brine, which has a lower freezing point and maximum density temperature. This brine is colder than the surrounding water, but sinks due to its density. This will affect the stability in the water, causing convective mixing not to be stable.

Another explanation to the difference in temperature measurements could be the calibration. An error in the hardware was found and a quick calibration solution had to be done. This calibration method may not have been accurate enough.

Figure 3.10 shows that the sensors in the tank bottom never measured a sufficiently cold temperature to activate the heating cables. This is a clear example of stabilized convective mixing. The highest density of freshwater is 4 °C, and the set point was 0 °C. All water with a higher density than water at 0 ° sank, preventing the bottom heating cables from being turned on since this is water of a higher temperature.

The plots of the temperature development in sea ice experiment 2 (fig. 3.20-3.22) show an indication of the temperatures measured stabilized after approximately 200 hours of ice growth. Possible reasons for this could be the ice thickness. The thickness causes the water temperature to become more stable since the amount of heat transfer decreases by increasing ice thickness. This could also be the explanation for temperature stabilizing not occurring in sea ice experiment 1, since it did not reach the same level of thickness.

Also it may be possible that the heating system can stabilize and dampen convective mixing when the heat flux through the ice is low. Low heat conduction slows down ice growth and production of brine pockets, which is the cause of convective mixing to be unstable.

The aim of the tank is to simulate one dimension ice growth processes. In reality it seems that there are horizontal gradients, and the size of the ice tank may be so small that the walls affect the hydrodynamics in the system.

After testing the equipment in 3 ice productions, the new system is showing significant improvement. The mentioned restrictions caused by the amplifications

and limited readings of the data acquisition device does not affect the equipment for the area of application. As assumed when creating the amplification circuit board.

4.2 Insulation

The previous version of the tank had inefficient insulation in some areas around the tank. A metal rod on the middle of the walls working as a perfect heat conductor caused ice growth along the submerged middle section of the tank. In addition, an old draining pipe located in the bottom of the tank conducted heat causing ice growth.

It was revealed when mounting new sensors under the tank that the insulation under the ice tank had shifted, resulting in no insulating effect. This was fixed and the insulation was mounted properly by using glue to prevent it from shifting again.

No submerged ice growth were longer observed after removing the old drain pipe, insulating all the walls with more polystyrene and mounting new wooden panels around the tank.

4.3 Computer program

The designed computer program showed good stability and the logging function was quite practical when performing calibration and testing of the heating system. The temperature development in the tank from sea ice experiment 2 show that the control engineering is working well. The results state that the chosen P-controller, and its parameters, were a suitable choice for this application.

The heating cables stopped working when the power was turned off. This is because the heating cables are powered by an outlet located inside the cold lab. But the temperature measurements did not stop, because the computer is stationed outside the lab and is powered by a separate outlet circuit. This suggests that the chosen solution of a computer controlled heating system is the best solution.

4.4 Ice thickness

Freshwater ice experiment

An ice block from the freshwater ice experiment is shown in figure 3.7. The block was located along one of the tank walls. The picture shows a horizontal ice sheet bottom and no indication of thicker ice growth along the tank wall.

A high water pressure under the ice was observed when the first sample of the ice was taken. The ice growth had lasted for 7 days and the ice had compressed the water, increasing the tank pressure. This effect is explained by freshwater ice not containing bubbles or channels that can release pressure, contrary to sea ice.

Sea ice experiment 1

The ice growth from sea ice experiment 1 shows a non-horizontal ice surface underneath the ice sheet by the walls (fig. 3.18). Angles of the bottom skewness was calculated to be $\approx 18°$, $18°$, $19°$ and $22°$; indicating that the thickness decreased approximately in the same rate from all four walls.

An interpolation was done based on the data from all samples taken from the ice sheet (fig. 3.19). The plot showed that the ice thickness was greatest at the back wall and in the left back corner. This was possibly caused by missing wood panels on the back wall. The old wood panels did not fit any longer after installing more insulation on the walls. Sea ice experiment 1 was conducted while waiting for carpenters to install new panels. However, some of the old panels were mounted (see fig. 4.1), in order to e.q. keep the terminal box on place. The plot also showed that the ice sheet had a more stable thickness in the area further than 20 cm from the walls.

Sea ice experiment 2

Ice blocks located by the walls from sea ice experiment 2 was shown in figure 3.27. This ice sheet did also not have a horizontal profile underneath. The blocks were taken from the same locations as in sea ice experiment 1, but this time bigger difference in skewness between the walls were detected. The left wall ice had a skewness of $\approx 11°$, while the front wall had a skewness of $\approx 21°$. The ice blocks at the left and right wall also had a skewness aligned with the wall, growing thicker towards the left- and right back wall corners.

This experiment had a 20 mm thick polystyrene covering the left half of the tank top cover (see fig. 4.1). This was done as a test attempting to prevent the

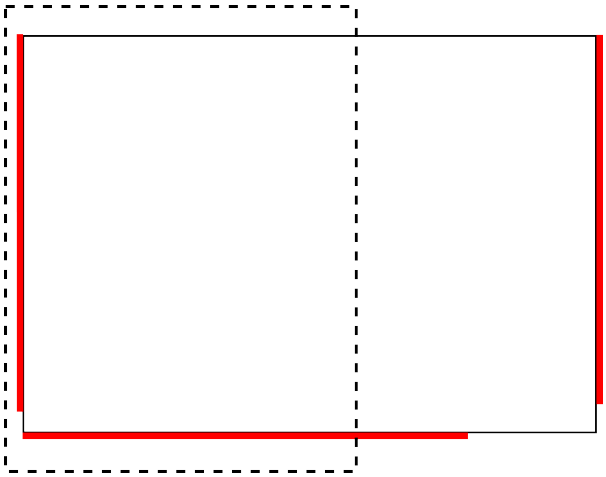

Figure 4.1: Illustration of tank during sea ice experiments. Red lines: wood panels mounted during sea ice Ex1. Dashed rectangle: polystyrene covering half the top during sea ice Ex2. Seen from above.

large ice growth that had been observed on this side in the previous experiment. This may have affected the ice thickness and could explain the small skewness angle under the ice by the left wall.

The contour plot of the ice thickness from sea ice experiment 2 shows that the thickest ice is at the top right corner, and not in the left back as in sea ice experiment 1. The 20 mm thick polystyrene is probably the cause of this. The new wooden panels were also mounted, so missing panels could not be the reason. This contour plot indicates an almost constant ice thickness in the area further than 20 cm from the walls.

Comparing all

The freshwater ice sheet did not show indication of skewness along the walls. This was the desired result when looking at the ice thickness. But when the sea ice experiments contained skewed ice, must the explanation be something else. The high water pressure was probably the reason, combined with the room temperature being -10 °C and not -20 ° as in the two other experiments.

The reason for the skewed ice growth in both sea ice experiments could be a combination of several factors. First of all, the inside walls of the tank are made

of metal. It has greater heat conduction than thick ice, which is one of the main reason for the skewness. But the skewness was not the same along every wall. A possible explanation of this is the location of the ice tank inside the cold lab. It is placed up in a corner with the back and right walls facing the lab walls, with a distance of ≈ 50 cm. The room cooling system is mounted in the ceiling. The system sucks warm air up from the middle and pushes cold air out along the ceiling making it come down along the walls. This could possibly cause cold air to be trapped in the corner between the tank and the lab walls, creating a pocket of colder air affecting these sides of the tank. The only way to look closer at this would be to move the tank and put it symmetrically under the cooling system and study the ice growth thusly.

The implementation of the test using polystyrene as cover may not have been done ideally. The test about the plate having any effect is inconclusive due to only the half of the tank is covered, which creates to many variables. But the results shows that its use might had a positive effect on the wall growth. The wooden cover plates should maybe be replaced with a large polystyrene plate to get a more conclusive result. This would of course affect the growth speed, but might also slow down the heat conduction effect of the metal walls. This is because the metal has to move the heat over the edge and not just up to the surface.

There is no data of previous ice thickness along the walls before the modifications were done. But the new ice thickness skewness is of a much smaller scale than the skewness observed last autumn. The old ice skewness could grow deep and get fused with the submerged ice which occurred due to the metal rod inside the walls.

4.5 Thin sections

Center of ice surface

When looking at the top horizontal thin sections from sea ice experiment 1 and 2, a clear difference can be seen. The grain sizes in the thin section from experiment 1 (fig. 3.14) is two to six times bigger than the grain sizes seen in the thin section from experiment 2 (fig. 3.24). A large amount of crystals seems to be oriented in the same direction, in both thin sections. This could be the crystals with a horizontal C-axis.

The vertical thin sections from sea ice experiment 1 (fig. 3.23) show a clear amount of columnar ice. This is S2 ice because the colours of the grains are different, due to crystal orientation. The wedge-out zone is located 2 cm down

in the ice sheet, which is much farther down compared to the location of the wedge-out zone in the ice sheet from sea ice experiment 2 (fig. 3.16). Here, it occurred before the ice became 1 cm thick. Columnar ice also occurred in this ice sheet, but with a smaller width than the columns in the first sea ice. The thin section shows that the columnar crystals were interrupted by larger horizontal crystals which stopped further growth of the columns. The cause of this is not clear, seeing as this experiment was conducted in the same way as the first sea ice experiment. Possible explanations could be that the process has been interrupted by a non-homogeneous saline mix in the tank, causing local temperature deviations under the ice. Crystals may have grown faster some places under the ice sheet, and then broken off and floated up under the ice sheet and then continued growing in the horizontal direction. It could also be an indication of a horizontal flow pattern under the ice sheet. A too high set point temperature in the tank could be a possible reason for such behaviour. Adjusting the temperature would possibly help preventing this.

The bottom horizontal thin sections from the ice sheet center did not carry many similarities. The thin section from sea ice experiment 1 (fig. 3.15) had a large amount of green colour, caused by crystals having a common orientation. The orientation of the crystals in the bottom thin section in experiment 2 (fig. 3.25) is more random which is probably caused by the interrupting horizontal crystals seen in the vertical thin section (fig. 3.23). However, a hint of alignment can be seen in the top left part of the thin section. This could be random or may be caused by a horizontal flow under the ice, causing crystals to align with the direction of flow.

Vertical thin sections along the wall

The presence of columnar ice along the tank wall was also examined. The thin section was made perpendicularly to the tank wall to see how the wall affected the ice crystals. A thin section from sea ice experiment 1 (fig. 3.17) shows that columnar ice occurred along the walls, though the columns did not grow vertically but perpendicularly to the skewed bottom of the ice sheet. The walls had influenced the growth, but columnar ice still occurred.

The vertical thin section perpendicular to the wall in sea ice experiment 2 did not have any columnar ice. But the grains showed an indication of the crystals' direction, which were the same as the columns seen by the wall in sea ice experiment 1. The reason columnar ice did not occur along the walls in sea ice experiment 2 is probably related to the same effects observed at the center of the same ice sheet.

5 Conclusion

This Master's thesis has examined an ice tank used for ice production in an NTNU cold lab. The tank was deemed inadequate to control the water temperature, and modifications were needed. The original temperature sensors were replaced with seven PT1000 sensors, with a measuring resolution of 0.1 °C. Two were placed on the bottom, two on the wall in the lower part and three on the upper part of the tank wall. The five sensors placed on the wall were mounted in a vertical line, so that a temperature profile could be measured in the water. The heating system was controlled by a computer program made by the author in LabVIEW. The program read the signals from the temperature sensors and uses control engineering to control the heating cables. The heating cables were powered by the use of three solid state relays, separating the tank into three sections; upper, lower and bottom. All software and hardware were developed by the author with guidance from staff at NTNU.

The new system was tested with three separate ice productions. One with freshwater ice and two with salt water ice (sea ice). Two elements were examined; ice thickness and temperature development. The ice thickness in the freshwater ice experiment was constant over the whole ice sheet, but this was probably a result of high water pressure underneath the ice. The ice sheets in the sea ice experiments were not horizontal, but thicker along the walls. The angle of the skewness ranged from 11° to 22° which was caused by several variables. The metal walls, which gave good heat conduction affected the growth. The use of a top cover with additional 20 mm polystyrene on the left side in one of the experiments clearly affected the ice thickness underneath this area. But the idea of a polystyrene cover might be better as a top cover than wooden plates, which is the current solution. The tank's position in the cold lab might also have an impact on the ice growth. The tank is placed in a corner, this might create a colder area behind the tank compared to other non-wall-facing sides of the tank. A experiment to test this would be to place the tank symmetrically under the cooling system and see if thicker ice growth still occurred.

The temperature profile in the freshwater ice experiment revealed that convective mixing had occurred, since the bottom sensors never measured a temperature lower than 0.1 °C. A repeating pattern was discovered in the temperature measurements. One sensor is often measuring 0.1 °C warmer than the other in each section of the tank. This could be a result of insufficient calibration, or there are local temperature deviations caused by convective mixing. A new and proper calibration must be made before this can be concluded.

The new heating system is a significant improvement from the previous set-up. A temperature profile can now be made, and all temperatures can be logged by the computer program. The highest placed sensor is close to the top edge, causing it to measure ice temperatures during production, which can be interesting in some experiments. The measured ice thickness along the walls is much smaller compared to the old tank. The ice sheet does still not have a constant thickness, but a significant improvement has been made.

The affect on the time spent on spraying, to initiate growth of columnar sea ice replication, has been examined. Two experiments were conducted; long spraying time and short spraying time. The long spraying was done in 16 minutes and 40 seconds. The result was columnar ice with a column width from 1-6 mm. Grains 9.8 mm under the surface was measured to be 3-5 mm wide, with a wedge-out zone approximately 2 cm under the surface.

The short spraying was conducted in 9 minutes and 15 seconds. The results gave columnar ice with a column width of 1-3 mm which is a significant difference from the long spraying test. The biggest difference was seen in the horizontal thin section, where the majority of crystals had a grain size smaller than 1 mm. The wedge-out zone also occurred much earlier in the growth process compared with the long spraying test. This coincides with the theory of wedge-out zones. When there is no more room in the horizontal direction, horizontal C-axis oriented crystals encapsulate other crystals preventing their continued growth.

Columnar ice was found along the tank walls in the long spraying test, but not in the short spraying test. This shows that a whole ice sheet of homogeneous structure can be produced in the tank. The fact that it did not occur in the short spraying test is probably caused by the disturbance that also had affected the columnar ice development in the center of the ice sheet, making it unrelated to the spraying time. The author would have conducted a new test of the second sea ice experiment in an effort to create continuously columnar sea ice, if more time had been available. Time was cut short due to a fire incident in the neighbouring

lab.

Results have shown that the time used on conducting the spraying when creating sea ice replicas has an impact on the resulting crystal sizes and how early the wedge-out zone will occur in the ice sheet.

6 Further work

Further work is to recalibrate the sensors. The proper way to do this is to create an ice bath in the whole tank, and not a comparing-method calibration like the one done in this thesis. The reason for this not being done in the first place was the lack of freshwater ice. This calibration method demands large amounts of freshwater ice, which takes weeks to produce.

Performing a new test of sea ice experiment 2, short spraying time. This to investigate whether the interrupted crystal growth would happen again, or if it just was a random incident.

Another interesting test would be to move the tank symmetrical under the cooling system and run a new ice growth test, in order to look at how the ice thickness along the walls develops.

More spraying tests can be done with different time windows, to see whether it is possible to find an expression describing the relation between spraying time and grain size. Possibly building an instrument that does the spraying instead of doing it manually.

Numerous new studies involving the tank can now be done, thanks to the possibility of controlling the temperature and monitoring the temperature profile with an accuracy of 0.1 °C. E.g., The first calibration test showed a very slow ice growth due to high water temperature. An interesting research topic revealed itself from this test; How much is the ice growth affected by small changes in water temperature?

Bibliography

[1] T.O. Myklebust. Properties and growth of laboratory made coulmnar saline ice. Project assignment, NTNU, 2013.

[2] N. Storey. *Electronics, A Systems Approach*. Pearson Education Limited, Essex, England, 4 edition, 2009.

[3] Crydom Inc., http://www.crydom.com/en/Products/Catalog/AdvancedWebPage.aspx. *Crydom ED24D3 Solid state relay*, 2014.

[4] M.S. Van Dusen. Platinum-resistance thermometry at low temperatures. *The bureau of standard united states department of commerce*, 47:326–332, 1925.

[5] RS, http://no.rs-online.com/web/p/platinum-resistance-temperature-sensors/2938446/. *PT1000 sensing element data sheet*, 2014.

[6] C. Wheatstone. The bakerian lecture: An account of several new instrumenst and processes for determining the constants of a voltaic circuit. *Philosophical Transactions of the Royal Society of London*, 133:303–327, 1843.

[7] A.R. Hambley. *Electrical Engineering, Principles and applications*. Pearson Education, Inc.

[8] Burr Brown, http://www.ti.com/product/INA125. *INA125, INSTRUMENTATION AMPLIFIER With Precision Voltage Reference*, 2014.

[9] Burr Brown, http://www.ti.com/product/INA126. *INA 126, MicroPOWER INSTRUMENTATION AMPLIFIER Single Versions*, 2014.

[10] ExpressPCB, http://www.expresspcb.com. *Express SCH*, 2014.

[11] Biltema Norge AS, http://www.biltema.no/no/Bygg/Kjemikalier/Ovrig/BT-Multibond-Rapid-364832/. *BT Mulitbond Rapid*, 2014.

[12] J.G. Balchenm, T. Andersen, and B.A. Foss. *Reguleringsteknikk*. Institutt for teknisk kybernitikk, NTNU, 2003.

[13] National Instruments, http://sine.ni.com/nips/cds/view/p/lang/no/nid/201987. *NI USB-6009*, 2014.

[14] H. Preston-Thomas. The international temperature scale of 1990 (its-90). *Metrologia*, 27:3–10, 1990.

[15] Ackley S.F. Weeks, W.F. *The growth, structure and properties of sea ice*. Plenum Press, New York, 1986.

[16] E.M. Sculson. At-332 physical environmental loads on arctic coastal and offshore structures. Lecture notes, The University Centre in Svalbard, UNIS, 2013.

[17] A. Assur. *Composition of sea ice and its tensile strength*. US Snow, Ice and Permafrost Research Establishment, 1960.

[18] Traco Power, http://www.tracopower.com/products/dc-dc-converters/sip-package/. *TMR 1-0522, DC/DC converters*, 2014.

[19] Loctite, http://www.loctite.no/tekniske-datablader-3910.htm. *Loctite 480, Technical datasheet*, 2014.

A Appendix

A.1 List of components and equipment used to modify tank

Components

- 7 Temperature sensors (PT1000) [5]
- Strip board
- 21 high precision 1000Ω resistors
- 1 INA125 [8]
- 6 INA126 [9]
- 7 high precision 200Ω resistors
- IC Socket adapters
- DC/DC converter [18]
- 2 capacitors, (0.1μF)
- 1 Transistor
- Channel connectors
- 3 Relays [3]

Equipment

- Aluminium plate
- Two-component glue
- Soldering stickers
- Wires of different dimensions
- Soldering equipment
- 4 core signal cable with shielding
- 16 core signal cable with shielding
- Plastic cap
- Glue, BT Multibond Rapid [11]
- Glue, Loctite 480 [19]
- Terminal box
- NI USB-6009 [13]
- Computer with LabVIEW
- Insulation(Glava EPS S 80 600x1200x20)
- Multimeter
- Different tools

A.2 List of equipment

Different equipment and tools used during lab work:

- **Scale**: AND, EK-400H, (SN: K9211955)
- **Salt**: JOZO, Havsalt 4kg
- **Salinometer**: METTLER TOLEDO, SevenGo conductivity meter SG3
  (SN: 1230265930, SN_{rod}: 5809042220)
- **Thermometer**: EBRO, TFX 422
  -50°C - +200C, (SN:15055760)
- **Power tool**: BOSCH, PSR 18 LI-2
- **Power tool**: Black and Decker, KR910
- **Sample cutter cylinder**: $\oslash$ = 71.5 mm
- **Air pump**: ABM, Typ.4EKF56CX-4, electrical motor
- **Microtome**: Leitz, 1400
- **Paraffin**: SHELL, Lampeolje
- **Caliper**: Cocraft
- **Polarized light device**: W. Ludolph, Typ: UDT87, (SN:56758)
- **Camera**: Canon EOS 650D, EF-S 15-85, (SN: 083033033606)
- Sieve to remove floating debris
- 3 spray bottles(0.7 L)
- Warm clothes
- Sample bottles
- Band saw
- Hand saw
- Garden hose
- Metal rod to measure ice thickness
- Ice tank
- Glass plates
- Measuring band
- Small brush
- Squeeze bottle w/ nozzle containing fresh water
- Different tools, screwdriver etc.
- Stop watch
- cold lab
- Plastic bags to store ice samples
- Stick to stir the water with

A.3 Pictures and data from Salt ice experiment 1

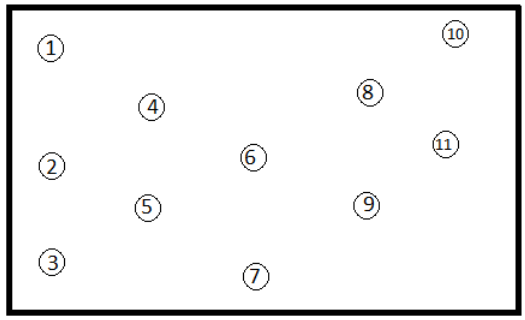

Figure A.1: Position of samples taken in tank from sea ice experiment 1, seen from above

Table A.1: Location and length of samples taken from sea ice experiment 1

Sample	X [cm]	Y [cm]	Thickness [mm]
1	8	72	147-160
2	8	39	100-120
3	11	10	100-120
4	38	52	80
5	38	30	73
6	62	45	61
7	64	9	76-90
8	86	59	65
9	85	29	64
10	111	72	100-120
11	113	36	80-100

Table A.2: Sample info from sea ice experiment 1, part 1 (all measures given in *mm*)

Samples	6 (61 mm)	4 (80 mm)	5 (73 mm)	8 (65 mm)	9 (64mm)
Location	Center	Center	Center	Center	Center
Top (Hor.)					
Part removed				8.6	7
Start thickness				18.6	20
Shaved off (from top)				2.2	2.8
Location of thin section from top				9.8	9.8
Thin section, thickness				0.9	0.5
Image file numbers				6654-6657	6677
Middle (Vert.)					
Location of thin section from top	Whole sample	Whole sample	Whole sample		
Thin section, thickness	0.4	0.4	0.55		
Image file numbers	6625	6634-6639	6646-6648		
Bottom (Hor)					
Part removed				6.7	6
Start thickness				14.2	24.5
Shaved off (from bottom)				3.4	3.3
Location of thin section from bottom				10.1	9.3
Thin section				0.5	0.4
Image file numbers				6658-6663	6688-6695

Table A.3: Sample info from sea ice experiment 1, part 2 (all measures given in mm)

Samples	1 (147-160 mm)	7 (76-90 mm)	11 (80-100 mm)
Location	Wall	Wall	Wall
Top (Hor.)			
Part removed			
Start thickness			
Shaved off (from top)			
Location of thin section from top			
Thin section, thickness			
Image file numbers			
Middle (Vert.)			
Location of thin section from top	75	Whole sample	Whole sample
Thin section, thickness	0.7	0.6	0.6
Image file numbers	6697-67001	6701-6705	6706-6721
Bottom (Hor)			
Part removed			
Start thickness			
Shaved off (from bottom)			
Location of thin section from bottom			
Thin section			
Image file numbers			

Pictures of ice blocks

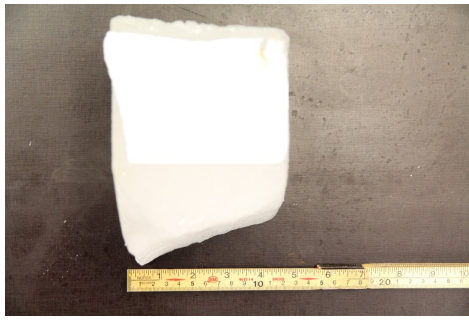

Figure A.2: Ice block 1

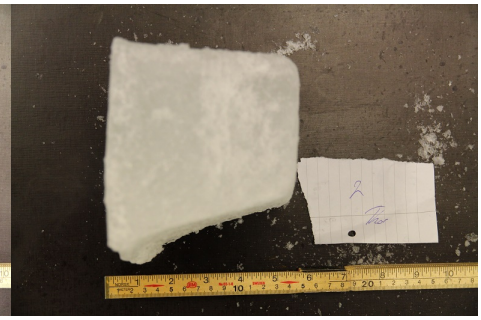

Figure A.3: Ice block 2

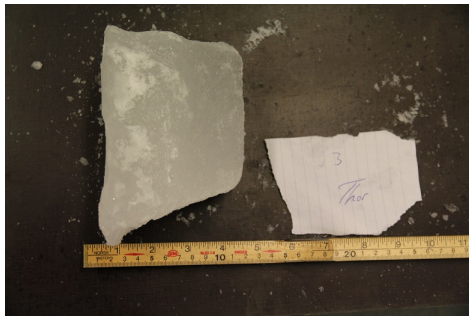

Figure A.4: Ice block 3

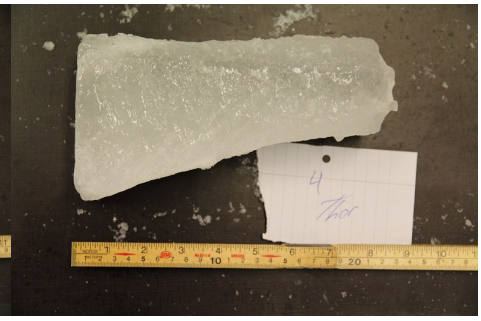

Figure A.5: Ice block 4

Thin Sections

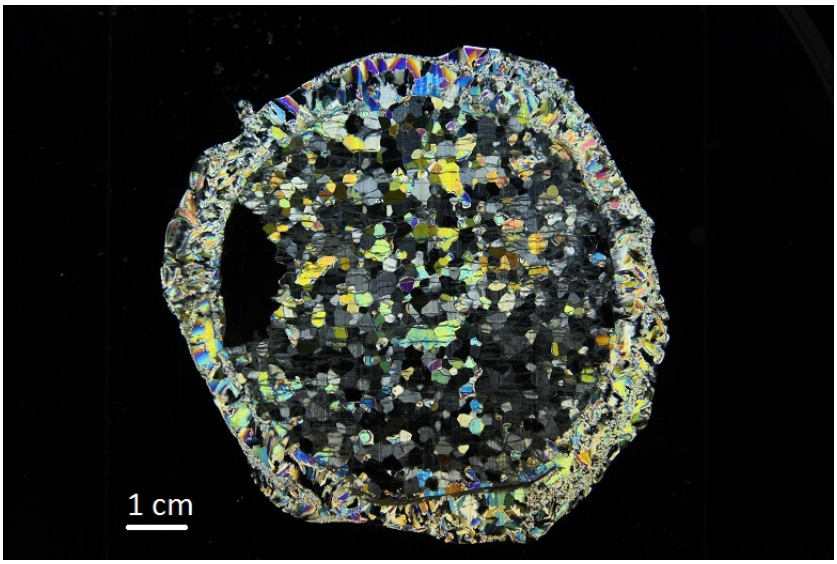

Figure A.6: Sample 8, Middle, Top.

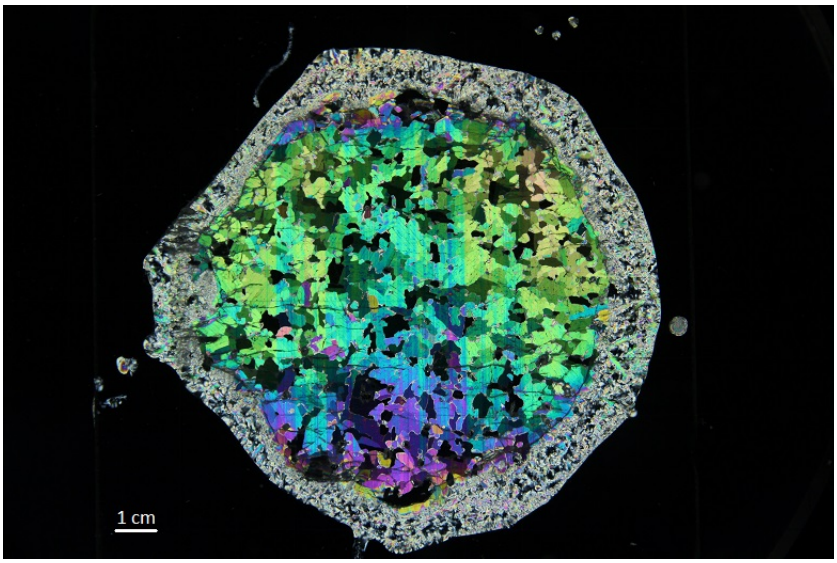

Figure A.7: Sample 8, Middle, Bottom.

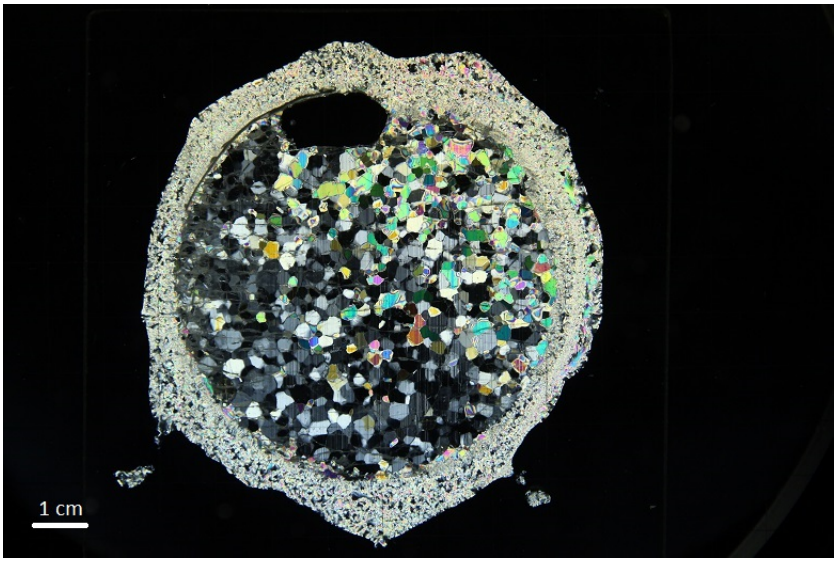

Figure A.8: Sample 9, Middle, Top.

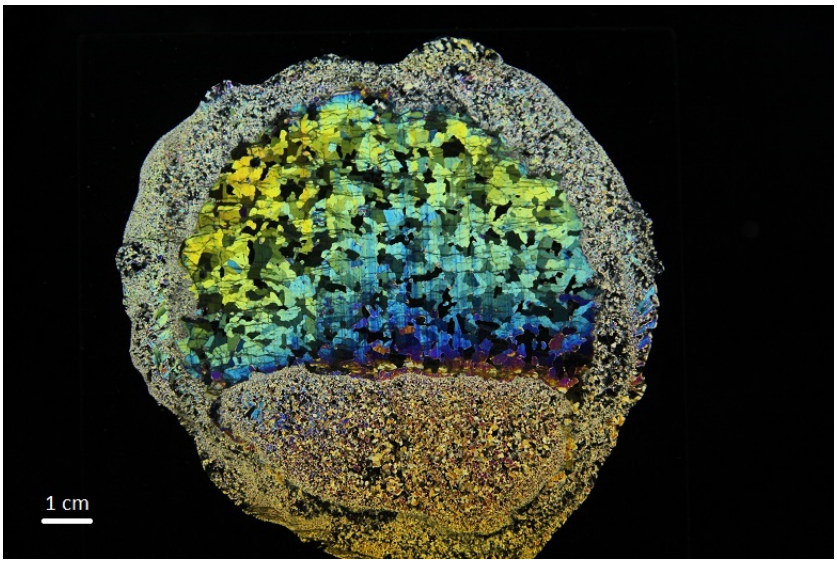

Figure A.9: Sample 9, Middle, Bot.

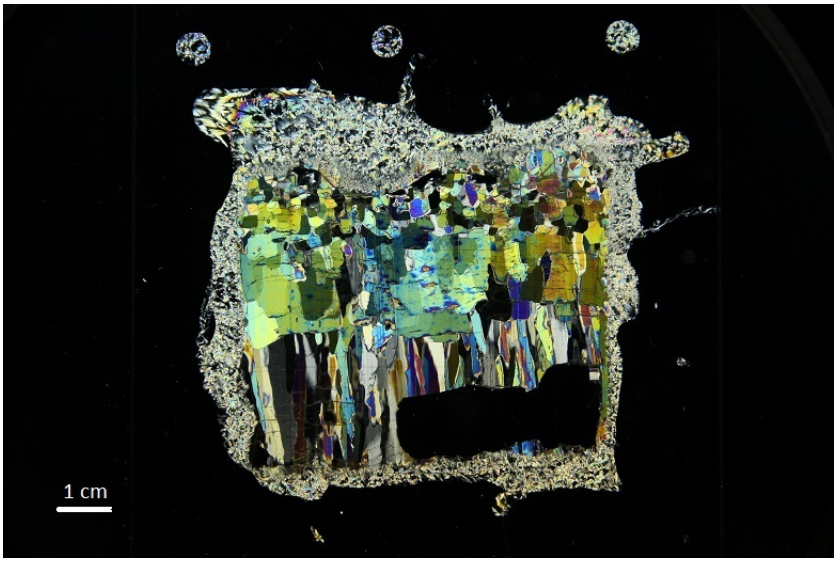

Figure A.10: Sample 6, Middle, Vertical.

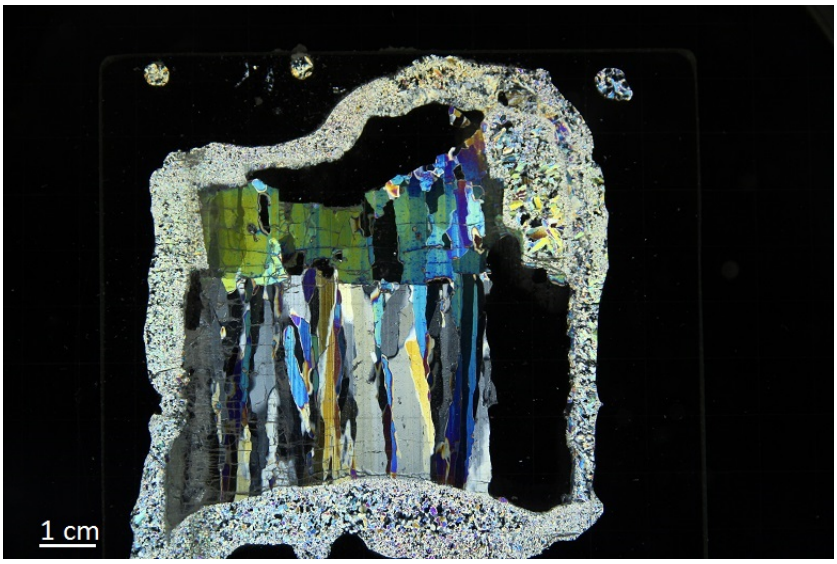

Figure A.11: Sample 4, Middle, Vertical.

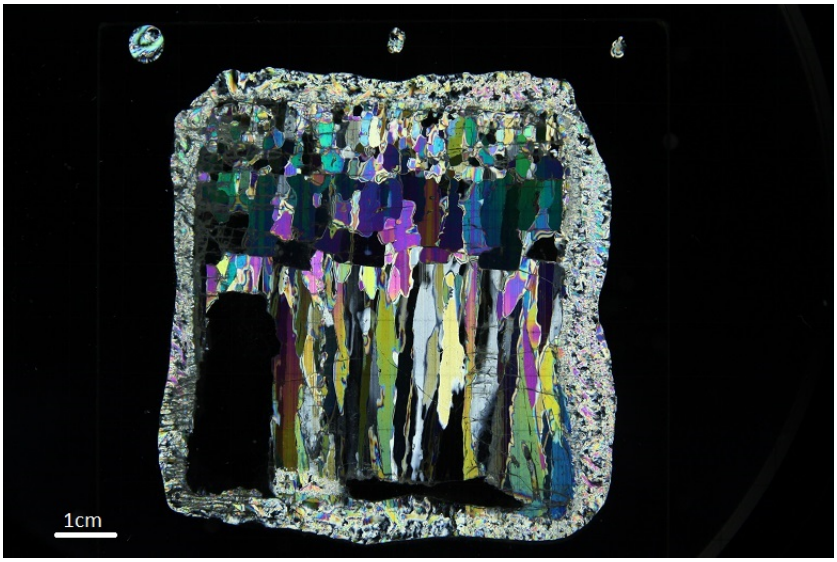

Figure A.12: Sample 5, Middle, Vertical.

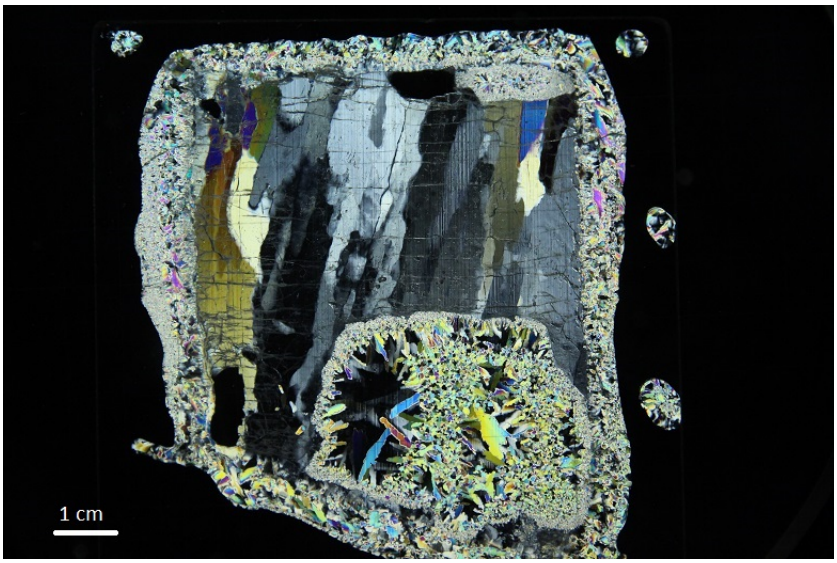

Figure A.13: Sample 1, Wall, Vertical.

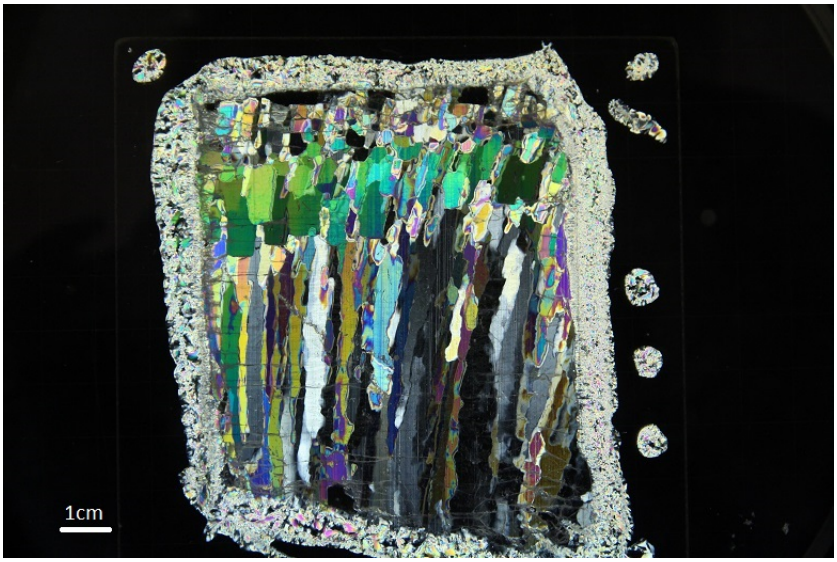

Figure A.14: Sample 7, Wall, Vertical.

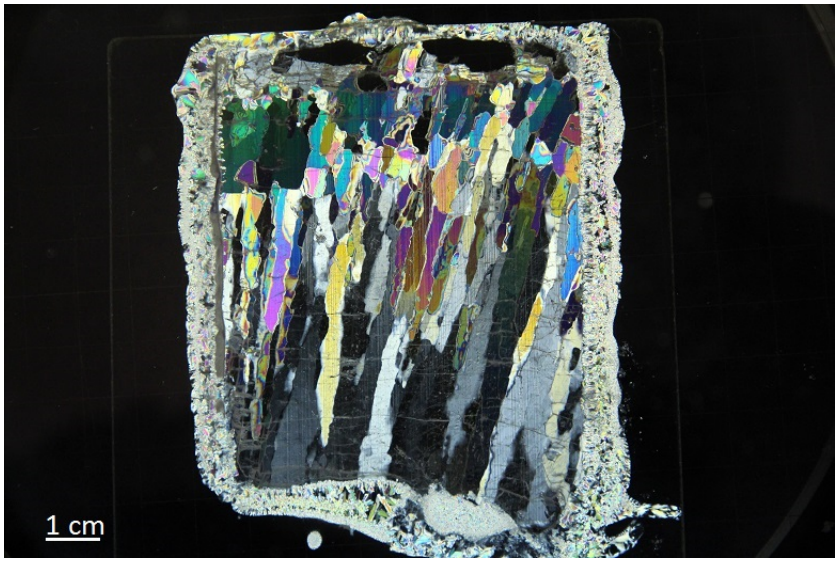

Figure A.15: Sample 11, Wall, Vertical.

A.4 Pictures and data from sea ice experiment 2

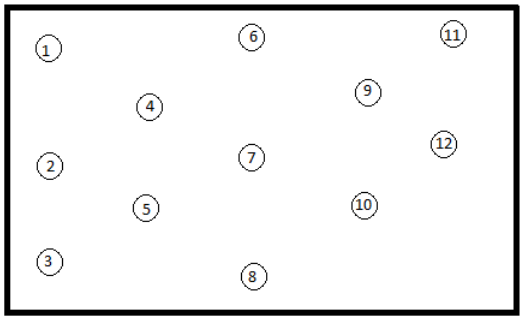

Figure A.16: Position of samples taken in tank from sea ice experiment 2, seen from above

Table A.4: Location and length of samples tank from sea ice experiment 2

Sample	X	Y	Thickness [mm]
1	8	62	173-195
2	8	41	170
3	9	17	100-120
4	35	53	110-120
5	35	29	100
6	55	71	129-150
7	58	44	950
8	58	11	112-135
9	85	53	126-138
10	85	27	130
11	110	64	200-220
12	110	38	170-190

Table A.5: Sample info from sea ice experiment 2, part 1 (all measures given in mm)

Sample	5 (100 mm)	7 (950 mm)	9 (126-138 mm)	4 (110-120 mm)	10(130 mm)
Location	Center	Center	Center	Center	Center
Top (Hor.)					
Part removed				7.6	9.6
Start thickness				18.3	20.4
Shaved off (from top)				2.9	2
Location of thin section from top				10.5	11.6
Thin section, thickness				0.5	0.5
Image file numbers				6760	6767
Middle (Vert.)					
Location of thin section from top	Whole sample	Whole sample	78		
Thin section, thickness	0.4	0.4	0.4		
Image file numbers	6751	6752	6757		
Bottom (Hor)					
Part removed				14.5	15
Start thickness				20	20.1
Shaved off (from bottom)				3.5	2.1
Location of thin section from bottom				18	17.1
Thin section				0.25	0.5
Image file numbers				6765	6772

Table A.6: Sample info from sea ice experiment 2, part 2 (all measures given in mm)

Samples	1 (173-195 mm)	8 (112-135 mm)	12 (170-190 mm)	6 (129-150 mm)
Location	Wall	Wall	Wall	Wall
Top (Hor.)				
Part removed				
Start thickness				
Shaved off (from top)				
Location of thin section from top				
Thin section, thickness				
Image file numbers				
Middle (Vert.)				
Location of thin section from top	105	42	86	54.5
Thin section, thickness	0.7	0.3	0.4	0.6
Image file numbers	6775	6779	6780	6787
Bottom (Hor)				
Part removed				
Start thickness				
Shaved off (from bottom)				
Location of thin section from bottom				
Thin section				
Image file numbers				

Thin sections

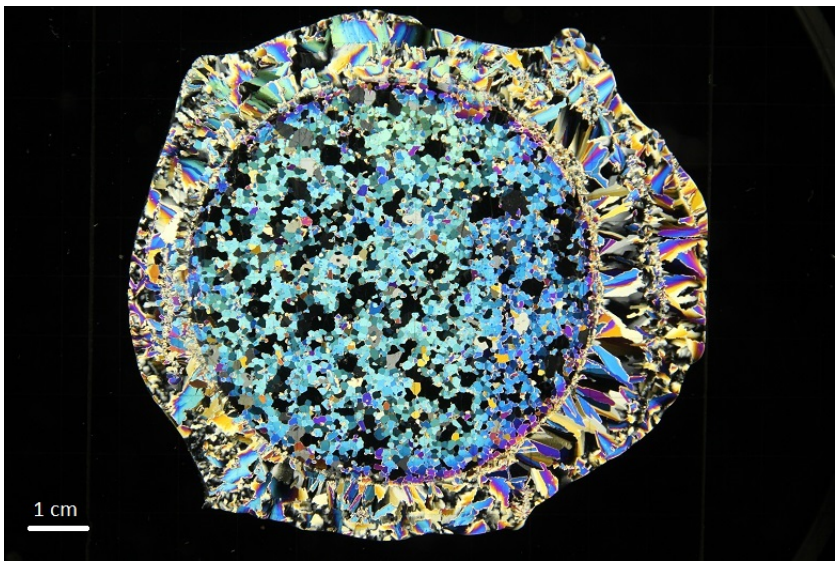

Figure A.17: Sample 4, Middle, Top.

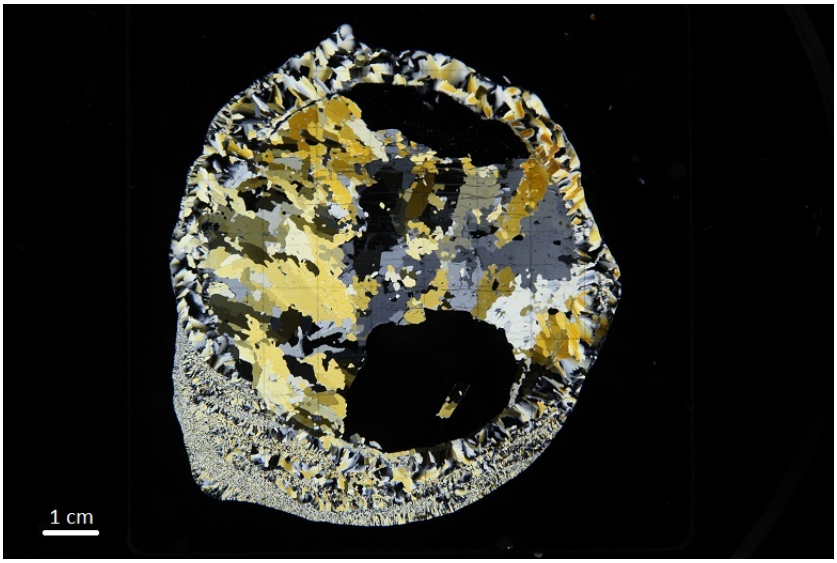

Figure A.18: Sample 4, Middle, Bot.

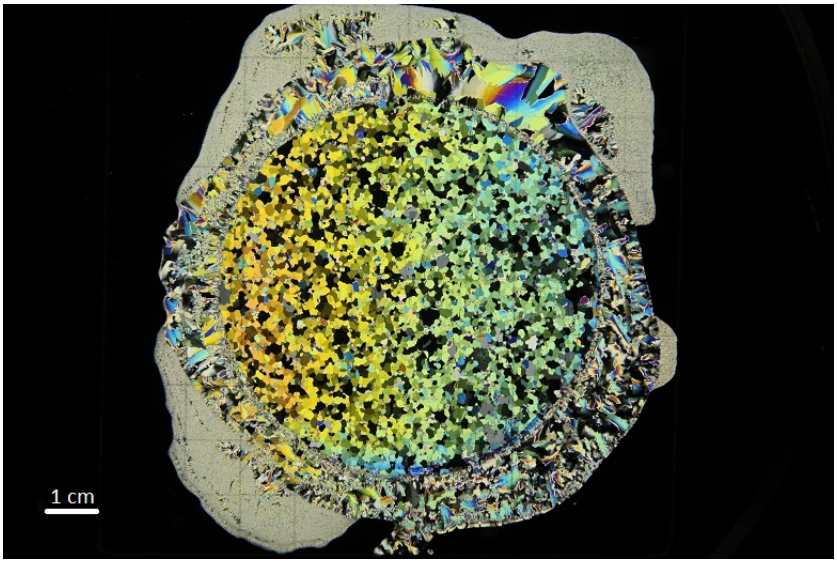

Figure A.19: Sample 10, Middle, Top.

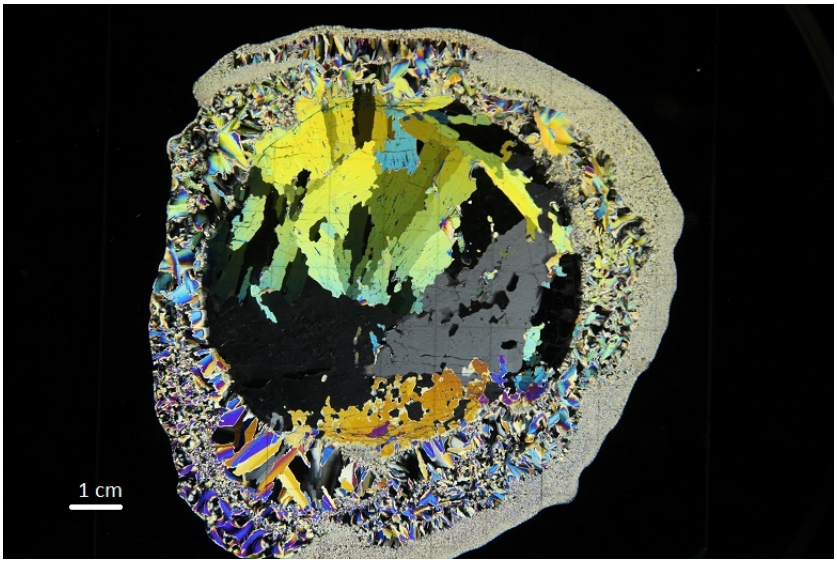

Figure A.20: Sample 10, Middle, Bot.

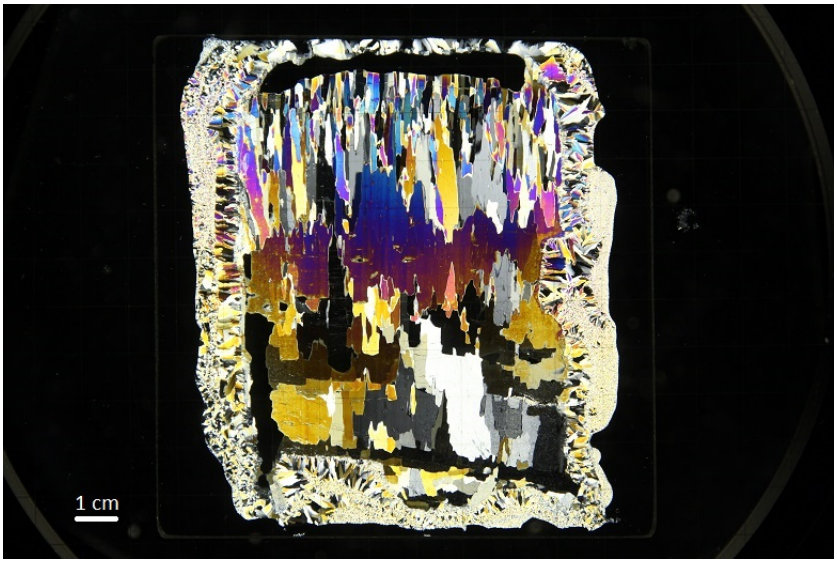

Figure A.21: Sample 5, Middle, Vertical.

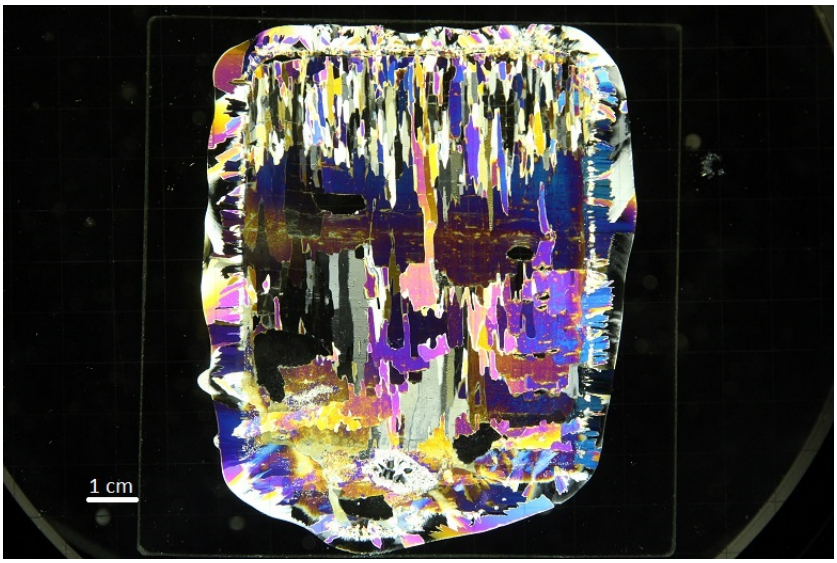

Figure A.22: Sample 7, Middle, Vertical.

Figure A.23: Sample 9, Middle, Vertical.

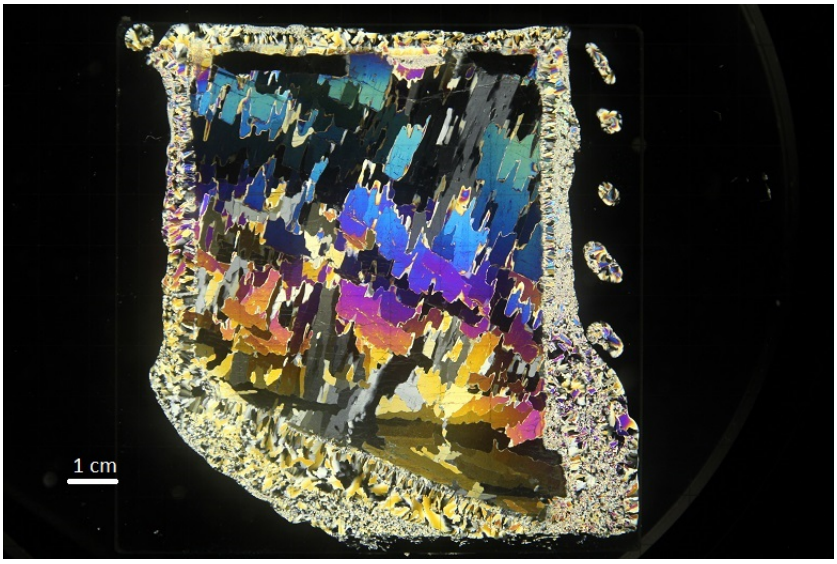

Figure A.25: Sample 8, Wall, Vertical.

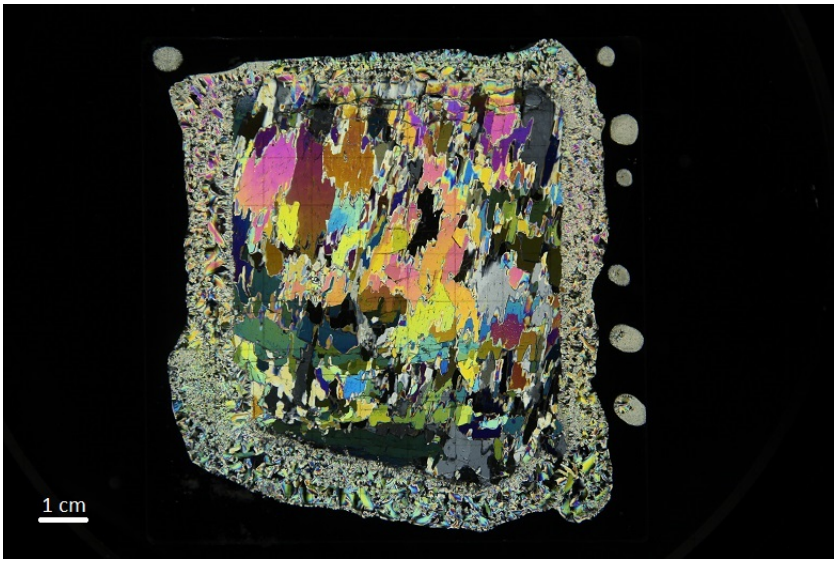

Figure A.24: Sample 1, Wall, Vertical.

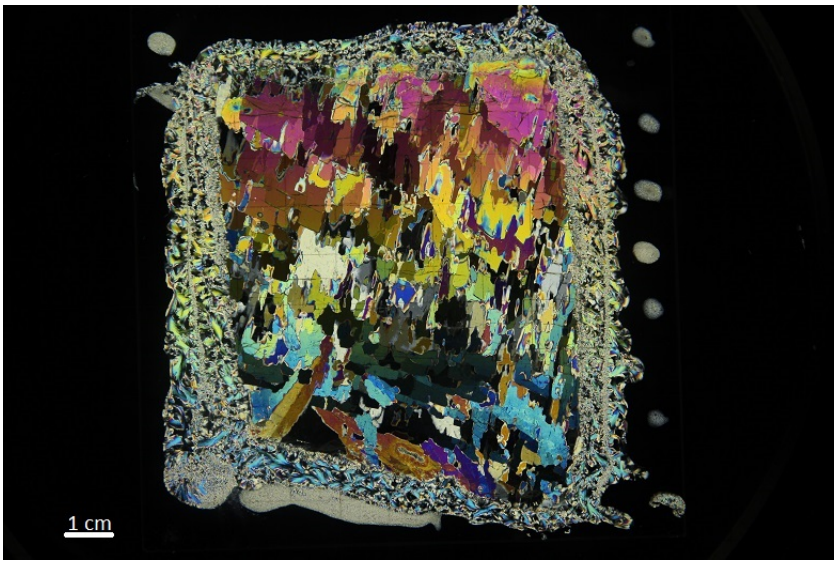

Figure A.27: Sample 6, Wall, Vertical.

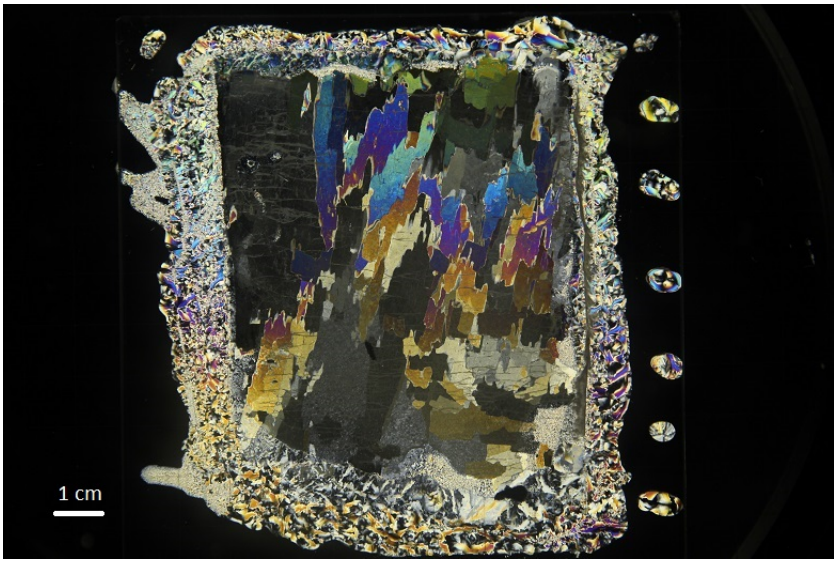

Figure A.26: Sample 12, Wall, Vertical.

Ice blocks

Figure A.28: Ice block 1

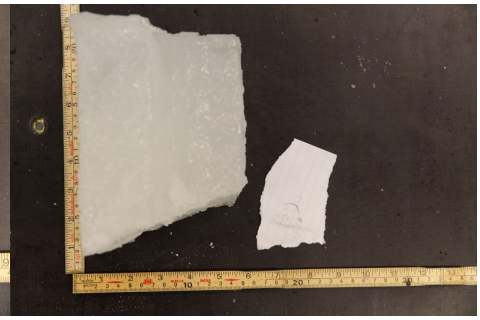

Figure A.29: Ice block 2

Figure A.30: Ice block 3

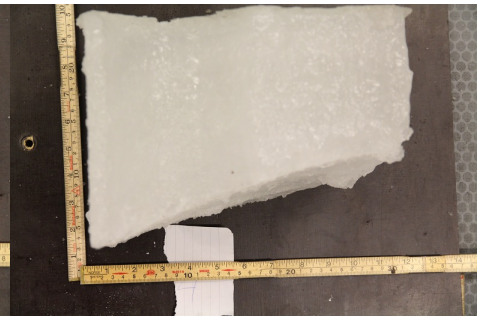

Figure A.31: Ice block 4

A.5 Tank set up. Sensor position and wiring diagram

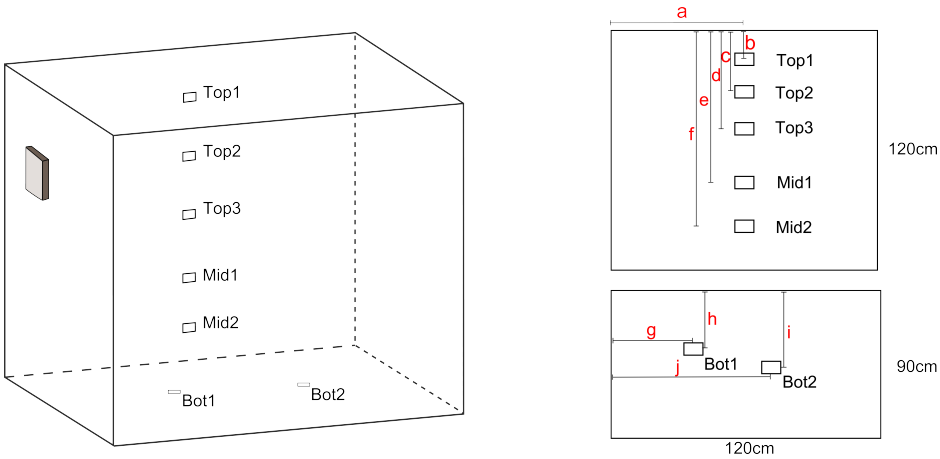

Figure A.32: Location of sensors. Measurements listed in table A.7.

Table A.7: Measurements of sensor locations seen in figure A.32.

Line	Length [cm]
a	62
b	22
c	44
d	57
e	79
f	104
g	46
h	32
i	46
j	87

Table A.8: Connection channels and color of signal cables.

Sensors & relays	Output channel on amplifier circuit	Signal cable colour	Connection port DAQ-device
Top1	Out2	Green	AI1
Top2	Out1	Blue-white	AI2
Top3	Out3	Yellow-white	AI3
Mid1	Out4	Orange-white	AI4
Mid2	Out5	Green-white	AI5
Bot1	Out6	Yellow	AI6
Bot2	Out7	Orange	AI7
-	+5V	Red, Red-white	+5
-	GND	Black-white	Ground
-	GND	Shielding	Ground (DC/DC conv.)
Top heating cable	-	Brown	P0.7
Middle heating cable	-	Grey	P0.5
Bottom heating cable	-	Blue	P0.6
Ground relay control	-	Black	+5